EPS-SG ICI Ice Water Path Product: ATBD

SAF/NWC/LEO-EPSSG/ATBD/IWP-ICI Issue 2.1, Rev. 2

Document Signature Table

	Name	Function	Signature	Date
Prepared by:	Bengt Rydberg	Möller Data Workflow Systems AB supporting NWCSAF		2016-09-29
Supported and reviewed by:	Patrick Eriksson	Chalmers University of Technology supporting NWCSAF		2016-09-30 2018-06-20
Reviewed by:	Vinia Mattioli	Microwave and Sub-Millimetre Scientist, Remote Sensing and Product Division, EUMETSAT		2016-12-01 2018-09-03
Reviewed by:	Christophe Accadia	Microwave and Sub-Millimetre Scientist, Remote Sensing and Product Division, EUMETSAT		2016-12-01
Reviewed by:	Anke Thoss	NWCSAF PPS Manager, SMHI		
Reviewed by:	Xavier Calbet	NWCSAF Scientific Coordinator, AEMET		
Authorised by:	Pilar Ripodas	NWCSAF manager, AEMET		

Document Change Record

Date/Issue	Remarks
2016-09-28/v1.0	Initial version of this ATBD. The ATBD is rewritten and replaces the old ATBD for the EPS-SG Ice Water Path Product from ICI v1.0
2016-12-07/v1.1	Modified text according to reviewer comments: - Added Sect. 1.3 : Applicable and reference document - Updated Table 2.1 according to latest EPS-SG EURD - Updated text about the definition of IWP in Sect. 2.1 - Moved text from Sect 3.1.1 to an added Sect 3.1.2: The importance sampling technique - Improved description about measurement vector and noise in Sect. 3.1.3 - Extended description of "Modify humidity" algorithm in Sect. 3.4.1 - Extended description of "Extract from database" algorithm in Sect. 3.4.2 - Extended description of retrieval algorithm output parameters in Sect. 3.5
2017-06-28/v2.0	Detailed description of submodules of retrieval algorithm that formerly was left for future updates: - additions and detailed specification of retrieval algorithm parameters in Sect. 3.3.4 - detailed description "obviously clearsky" algorithm in Sect. 3.4.1 - detailed description "Channel selection" algorithm in Sect. 3.4.2 - detailed description of "extract from database" algorithm in Sect. 3.4.2 Verification of retrieval algorithm by apllication to GMI observations (Appendix B) Additions of new parameters in retrieval database file (Appendix A) Addition of a system observation noise term that reflect error in forward modelling of surface contribution
2017-11-27/v2.0	Modified text according to reviewer comments: - updated description of ICI geophysical products (Sect. 2.2) - updated Fig. 3.1 - updated Eq. 3.4 and Eq. 3.7 and associated text - added a new section (Sect. 3.2), that describes ICI retrieval errors and performance - added a new conceptual figure (Fig. 3.5), and updated associated text describing the "obviously clearsky" module

Continued on next page

– continued from previous page

Date/Issue	Remarks
	- updated Fig. 3.6 (formerly Fig. 3.4). The figure now more clearly describes that the algorithm has two iteration counters - updated text in Table 3.3 and 3.4 to better describe the retrieval algorithm parameters, modified the "surface wind speed max diff" parameter relevant for "extract from database" module to now be a list containing one value for ocean pixels and one value for non ocean pixels - updated text in Sect. 3.5.1 and 3.5.2 to better describe sub-modules of the retrieval algorithm
2018-06-21/v2.1	Revised and modified description of retrieval algorithm: - a surface type fraction and mask (water, ice, snow, mixed, land) is calculated in *Extract ECMWF and surface data* (Sect. 3.4.1) - special treatment of observation associated with a mixed surface type is described in *RTTOV* (Sect. 3.4.1) - *Channel selection* (Sect. 3.4.1) now takes into account of four different surface types (water, ice, snow, mixed, land) - an iterative scheme is deployed in *Extract from database* (Sect. 3.4.2) - a refined expression is used in *Check weights* (Sect. 3.4.2) - channels are described to be removed in an order according to atmospheric opacity (*Remove channels*, Sect. 3.4.2) - *New channel selection* algorithm is slightly modified (Sect. 3.4.2) Changes in algorithm input: - dynamic parameter sea ice concentration added (Sect. 3.5.3) - new retrieval algorithm parameters, related to surface type, are introduced Moved description of retrieval database generation method into Appendix A Added Appendix B (retrieval performance sensitivity)
2018-12-21/v2.1	Modified text according to reviewer comments: - updated description of ICI geophysical products (Sect. 2.2) - corrected typo in Eq. 3.4 - more detailed description of retrieval accuracy and uncertainty in Sect. 3.2 - more detailed description of the *Extract from database* (Sect. 3.4.2) part of the retrieval algorithm

Contents

Chapter 1

Introduction

1.1 Purpose of this document

The Ice Cloud Imager (ICI) is an upcoming instrument that will be a component of the European Organization for the Exploitation of Meteorological Satellites (EUMETSAT) Polar System (EPS) Second Generation (EPS-SG). One of the objectives of ICI is to provide an ice water path (IWP) product.

The ICI IWP operational retrieval algorithm needs to be both correct and capable of processing large quantities of data in near real time. The retrieval algorithm must also consider that the retrieval problem is non-unique and non-linear, and that cloud properties exhibit non-Gaussian statistics.

A retrieval algorithm based on a retrieval training database has earlier been proposed and shown to be suitable for this task. The training database is the most crucial element of the ICI retrieval algorithm. The training database consists of a sufficiently large set of atmospheric scenes, along with associated (simulated) measurements. The physics and variability must be representative of the real world, as it will be used by the retrieval algorithm to perform the mapping from measurements to IWP. The retrieval algorithm will basically perform the wrong mapping if the training data are not sufficiently correct.

The ICI retrieval algorithm follows a Bayesian methodology, i.e. it has a clear link to probability theory and an error estimate is provided for each individual retrieval. The retrieval algorithm contains also a number of sub-algorithms and parameters in order to make the algorithm computational efficient and adjustable to issues that might appear in the operational phase. The purpose of this Algorithm Theoretical Basis Document (ATBD) is to describe the details of the ICI retrieval algorithm and the data required to produce the ICI IWP product.

1.2 Structure of this document

Section 2 of this document provides a short overview of the EPS-SG ICI instrument characteristics and the IWP product. This is followed, in Section 3, by a description of the basis of the retrieval algorithm, estimated retrieval performance, the details of the component of the retrieval processing chain, and the algorithm input and output data. Suggestions of future

work are presented in Section 4. A full list of acronyms is provided in Section 1.4. Literature references are listed in the end of this document.

Furthermore, the document contains a number of appendices. Appendix A provides a description of important aspects of the retrieval database and a method how such a database can be generated, including a sanity check of the database. Appendix B describes retrieval performance sensitivty to some of the algorithm parameters. The described retrieval algorithm has been applied on observations from Global Precipitation Measurement (GPM) Microwave Imager (GMI) and ISMAR (International SubMillimetre Airborne Radiometer) in order to verify that the retrieval algotithm provides sound results (Appendix C). GMI is probably the most similar satellite instrument to ICI that is in service today, and ISMAR basically is an air borne demonstrator instrument for ICI. ISMAR has been flown together with other instruments on the FAAM BAe-146 research aircraft.

1.3 Applicable and reference document

Table 1.1 lists documents that have been used to establish this document.

Table 1.1: Applicable and reference document.

Doc ID	Title	Reference
[EURD]	EPS-SG End Users Requirements Document	*EUM/PEPS/REQ/09/0151*
[SRD]	EPS-SG System Requirements Document	*EUM/LEO-EPSSG/SPE/13/735903*

1.4 Acronyms and Definitions

Table 1.2 lists definitions for all acronyms used in this document.

Table 1.2: Acronyms and Definitions.

Notation	Description
ANN	Artificial Neural Network
ARTS	Atmospheric Radiative Transfer System
ATBD	Algorithm Theoretical Basis Document
ATMS	Advanced Technology Micirowave Sounder
BMCI	Bayesian Monte Carlo Integration
CPR	Cloud Profiling Radar
DDA	Discrete Dipole Approximation
EPS	EUMETSAT Polar System
EPS-SG	EPS Second Generation
ERA	ECMWF Re-Analysis
ECMWF	European Centre for Medium-range Weather Forecasting
GPM GMI	Global Precipitation Measurement (GPM) Microwave Imager (GMI)
ICI	Ice Cloud Imager
ISMAR	International Sub-Millimetre Airborne Radiometer
IWC	Ice Water Content
IWP	Ice Water Path
LWC	Liquid Water Content
MARSS	Microwave Airborne Radiometer Scanning System
NWCSAF	NoWCasting Satellite Application Facility
PSD	Particle Size Distribution
RH	Relative Humidity
RTM	Radiative Transfer Model
SSP	Single Scattering Properties
SMHI	Swedish Meteorological and Hydrological Institute

Chapter 2

Ice Cloud Imager

2.1 Relevant instrument characteristic

The Ice Cloud Imager (ICI) is a conically scanning, with an incidence angle of 53°, millimetre/sub-millimetre wave radiometer, providing a total number of 13 channels (including dual polarization channels). Table 2.1 shows specification of the ICI channels. The ICI frequency coverage is from 183 GHz up to 664 GHz, with two window channels (243 GHz and 664 GHz) measured at both V and H polarization. The remaining channels are located around three different water vapor transition lines (around 183 GHz, 325 GHz, and 448 GHz). ICI has a 16 km on-ground footprint at all frequencies.

2.2 Geophysical products

The primary product of ICI is Ice Water Path (IWP;[kg/m^2]). We here define IWP as the field of view (FOV) weighted vertical column of atmospheric ice, including cloud ice, graupel, snow, and hail, along the slant direction, i.e:

$$IWP = \int_{FOV} \int_{s_0(z(s)=z_1)}^{s_1(z(s)=z_0)} a(\Omega) cos(\theta_{inc}) IWC\left(z(s), \delta(s), \lambda(s)\right) ds^{'} d\Omega^{'} \tag{2.1}$$

where a is the normalized antenna response function, $d\Omega = sin\theta d\theta d\phi$ is an element of solid angle, IWC is the ice water content [kg/m^3] that varies with altitude (z), latitude (δ), and longitude (λ), s denotes the distance from the sensor along a viewing direction (θ and ϕ), and θ_{inc} is the incidence angle (this gives that IWP=1 kg/m^2 for a state having a 1 km vertically thick homogeneous layer of IWC of 10^{-3} kg/m^3, and that covers the view of ICI). The integration or altitude limits z_0 and z_1 denote an altitude in the lower and upper part of atmosphere, respectively (current value of z_0 and z_1 is 0 km and top of the atmosphere, respectively). It is natural to define z_0 as 0 km above the surface, but the retrieval of cloud properties near the surface is problematic. This means that the ICI IWP product could potentially be more accurate if z_0 is defined at a higher altitude. However, the current definition of z_0 is not anticipated to be changed for the ICI IWP product.

Table 2.1: ICI instrument characteristic.

Channel	Frequency [GHz]	NEΔT [K]	Bias [K]	Polarization	Footprint Size at 3 dB [km]
ICI-1	183.31 ± 7.0	0.8	1.0	V	16
ICI-2	183.31 ± 3.4	0.8	1.0	V	16
ICI-3	183.31 ± 2.0	0.8	1.0	V	16
ICI-4	243.2 ± 2.5	0.7	1.5	V, H	16
ICI-5	325.15 ± 9.5	1.2	1.5	V	16
ICI-6	325.15 ± 3.5	1.3	1.5	V	16
ICI-7	325.15 ± 1.5	1.5	1.5	V	16
ICI-8	448.0 ± 7.2	1.4	1.5	V	16
ICI-9	448.0 ± 3.0	1.6	1.5	V	16
ICI-10	448.0 ± 1.4	2.0	1.5	V	16
ICI-11	664.0 ± 4.2	1.6	1.5	V, H	16

A second retrieval product is the mean mass height (Z_{mean};[m]), defined as

$$Z_{mean} = \frac{\int_{FOV} \int_{s_0(z(s)=z_1)}^{s_1(z(s)=z_0)} a(\Omega) cos(\theta_{inc}) z(s) IWC\left(z(s), \delta(s), \lambda(s)\right) ds' d\Omega'}{IWP} \tag{2.2}$$

which only is relevant if IWP $> 0\,\mathrm{kg/m^2}$.

A third retrieval product (also only relevant if IWP $> 0\,\mathrm{kg/m^2}$) is a cloud ice particle characteristic size, the mean particle size by mass (D_{mean};[m]). The cloud particle size distribution, PSD, can be described as a function of the mass equivalent spherical diameter D_{eq}, and that gives that $IWC \sim \int D_{eq}^3 n(D_{eq}) dD_{eq}$ where we denote the PSD as $n(D_{eq})$ ($[\#/\mathrm{m^4}]$), and we further define D_{mean} as the IWC weighted mean D_{eq}, i.e.

$$D_{mean} = \frac{\int_0^\infty D_{eq}^4 n_{av}(D_{eq}) dD_{eq}}{\int_0^\infty D_{eq}^3 n_{av}(D_{eq}) dD_{eq}}, \tag{2.3}$$

where $n_{av}(D_{eq})$ describes the PSD of the sampled atmospheric volume, weighted by the antenna response, by ICI,

$$n_{av}(D_{eq}) = \frac{\int_{FOV} \int_{s_0(z(s)=z_1)}^{s_1(z(s)=z_0)} a(\Omega) cos(\theta_{inc}) n\left(D_{eq}, z(s), \delta(s), \lambda(s)\right) ds' d\Omega'}{z_1 - z_0}. \tag{2.4}$$

Chapter 3

Retrieval algorithm for ICI

3.1 Retrieval algorithm basis

The aim of this section is to describe the basis of the ICI retrieval algorithm. Figure 3.1 shows a high level overview of the input and output data of the ICI retrieval algorithm.

The ICI Level2 algorithm is a Monte Carlo integration implementation. A core part of the retrieval algorithm is a retrieval database file, that contains a discrete representation of possible atmospheric states and corresponding simulated measurements. Effectively, the retrieval algorithm interpolates between database states that match a given measurement. More specifically, weights (or probability estimates) are calculated for each database state, where the weight depends on the deviation between radiances of the observation and database state and on the observation system noise. From these weights and database atmospheric states best estimates and uncertainties of retrieval variables can be derived.

The basis of the Monte Carlo integration retrieval algorithm is desbribed in Sect. 3.1.1, Sect. 3.1.2, Sect. 3.1.3, and Sect. 3.1.4, while the details of the actual ICI Level2 retrieval algorithm implementation, including the inputs and outputs, are described in Sect. 3.4, Sect. 3.5, and Sect. 3.6. Limitations of the retrieval algorithm is described in Sect. 3.3.

3.1.1 Retrieval problem and Monte Carlo Integration

Three basic considerations are that the retrieval problem is non-unique and non-linear, and that cloud properties exhibits non-Gaussian statistics. Since a priori information to handle the non-uniqueness aspect exists, a Bayesian retrieval approach is suitable. Following the Bayes theorem, the conditional expected value of the state vector ($\hat{\mathbf{x}}$) can be retrieved as

$$\hat{\mathbf{x}} = \int \mathbf{x} P(\mathbf{x}|\mathbf{y}) d\mathbf{x} = \frac{\int \mathbf{x} P(\mathbf{y}|\mathbf{x}) P(\mathbf{x}) d\mathbf{x}}{P(\mathbf{y})}, \tag{3.1}$$

where $\mathbf{y}$ is the measurement vector, $P(\mathbf{x}|\mathbf{y})$ is the conditional probability density function (PDF) of $\mathbf{x}$ given $\mathbf{y}$, $P(\mathbf{x})$ is the prior PDF of $\mathbf{x}$, $P(\mathbf{y}|\mathbf{x})$ is the conditional PDF of $\mathbf{y}$ given $\mathbf{x}$, and $P(\mathbf{y})$ is the prior PDF of the measurement. A direct application of Eq. 3.1 would require an integration over the whole state space, which in practice is a too demanding operation for the application on ICI measurements.

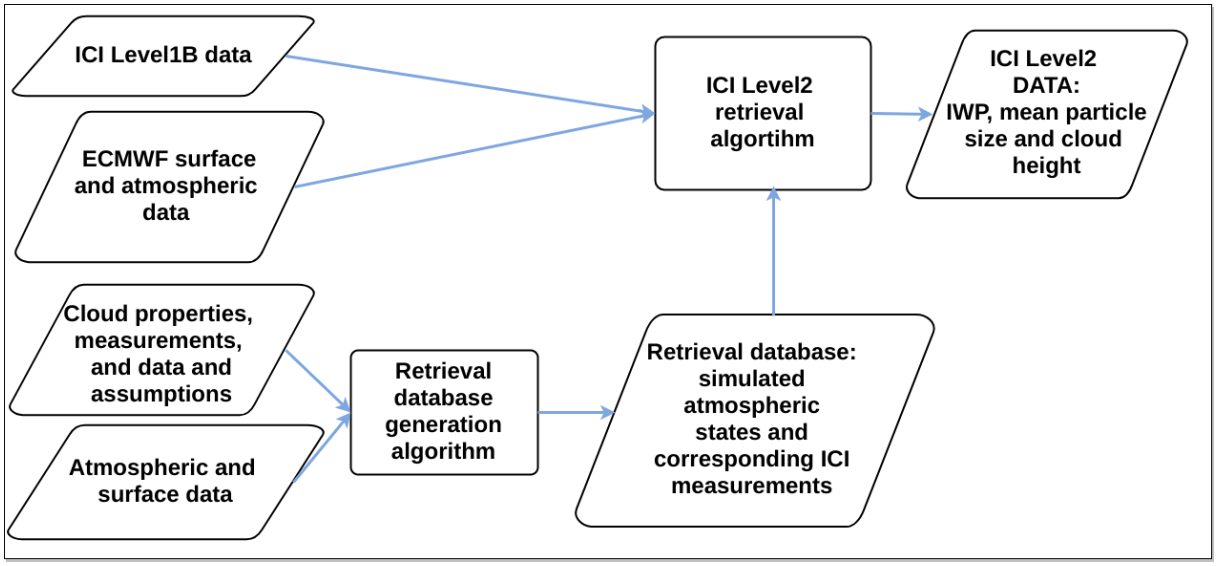

Figure 3.1: A high level description of input/output data of the ICI retrieval algorithm.

Several methods can be applied to solve Eq. 3.1. Two such methods are Artificial Neural Nets (ANN) [Jiménez et al., 2007] and Bayesian Monte Carlo integration (BMCI) [Evans et al., 2002]. The BMCI and ANN methods both make use of a discrete representation of the state and measurement spaces through a retrieval database (Appendix. A), in order to approximately solve Eq. 3.1. A common requirement for applying BMCI and ANN is that a retrieval database matching reality with sufficient accuracy must be created. The ANN application involves a second critical step where a mapping function is derived. This can potentially result in information being lost.

The BMCI method has been selected due to its conceptual clarity and direct link to probability theory. In the BMCI method Eq. 3.1 is solved practically by transforming it into a Monte Carlo integration

$$\hat{\mathbf{x}} \approx \frac{\sum_i \mathbf{x}_i P(\mathbf{y}|\mathbf{x}_i)}{\sum_i P(\mathbf{y}|\mathbf{x}_i)} \tag{3.2}$$

where the summation is performed over states $\mathbf{x}_i$, of the retrieval database, sampled from $P(\mathbf{x})$. From Eq. 3.2 it is clear that the retrieved state is a weighted average over all states in the database. In Sect. 3.1.2 it is described how Eq. 3.2 can be formulated in a more efficient way for the ICI application. The weight, $P(\mathbf{y}|\mathbf{x}_i)$, of each state depends on the noise of the measurement and how closely the simulated measurement is to the actual measurement. If one assumes that the noise of the observation is distributed in a Gaussian manner, which is often an adequate approximation, then $P(\mathbf{y}|\mathbf{x}_i)$ can be expressed as

$$P(\mathbf{y}|\mathbf{x}_i) \sim exp\left(-\frac{(\mathbf{y}-F(\mathbf{x}_i))^T(\mathbf{S}_o+\mathbf{S}_s)^{-1}(\mathbf{y}-F(\mathbf{x}_i))}{2}\right), \tag{3.3}$$

where $F(\mathbf{x}_i)$ is the simulated measurement vector for state $\mathbf{x}_i$ and $\mathbf{S}_o$ and $\mathbf{S}_s$ is the measurement and simulation error covariance matrixes, respectively. The observation system noise terms are described in more details in Sect. 3.1.3.

3.1.2 The importance sampling technique

In the preceding section it was described how a BMCI technique can be used to solve Eq. 3.1, through sample states from $P(\mathbf{x})$. This is known as an importance sampling technique. It is not a necessity to sample from $P(\mathbf{x})$ in order to solve Eq. 3.1, as the theory of importance sampling technique allows one to sample from almost any PDF. Although, $P(\mathbf{x})$ is the most natuarl choice of PDF to sample from, it is in practise not the most efficient one for the ICI application, as will be described below.

The retrieval database must in practice, clearly, contain a finite number of states. A problem with a direct application of Eq. 3.2 for the ICI application is that the most likely state is clear sky (here IWP $= 0\,\mathrm{kg/m^2}$). This means that a retrieval database sampled from $P(\mathbf{x})$ mainly contains clear sky states, that for a measurement containing a clear cloud signal, have insignificant contributions to the integral. The retrieval calculation can then potentially be both computational expensive and inaccurate (in the case that only a few states have a significant contribution).

One way to overcome this problem is to chose a different PDF ($G(\mathbf{x})$) from where the states are sampled, and apply an appropriate weighting compensating for the selected distribution while solving the integral. That is, Eq. 3.2 can be rewritten as

$$\hat{\mathbf{x}} \approx \frac{\sum_i \mathbf{x}_i P(\mathbf{y}|\mathbf{x}_i)}{\sum_i P(\mathbf{y}|\mathbf{x}_i)} \approx \frac{\sum_j a_j \mathbf{x}_j G(\mathbf{y}|\mathbf{x}_j)}{\sum_j a_j G(\mathbf{y}|\mathbf{x}_j)}, \tag{3.4}$$

where the summation (on the right hand side) now is performed over states $\mathbf{x}_j$ sampled from $G(\mathbf{x})$, and the weight a_j, which we refer to as an *a priori* weight, depends on both $P(\mathbf{x})$ and $G(\mathbf{x})$. In principle, the sampling can be performed from any PDF given that it is possible to sample from it, and that the correct compensating weighting can be derived. The latter is in general not trivial for the ICI application.

A fairly straight forward application of the importance sampling technique for the ICI application is to sample from a PDF $G(IWP)$ where the probability for IWP$=0\,\mathrm{kg/m^2}$ is lower than according to the true PDF $P(IWP)$, but otherwise is identical to $P(IWP)$. It is then intuitively clear that the sampled states with IWP $= 0\,\mathrm{kg/m^2}$ must be given a higher weight when solving the integral. In practice the sampling from $G(IWP)$ can be realized by sampling from $P(IWP)$ but only accepts states with IWP $= 0\,\mathrm{kg/m^2}$ with a desired probability p_0. In this case we have that

$$a_j = P(IWP)/G(IWP) \begin{cases} = 1 & \text{if IWP} > 0 \\ = 1/p_0 & \text{if IWP} = 0 \text{ and } 0 < p_0 \leq 1. \end{cases}$$

The approach described above can significantly reduce the required number of states in the retrieval database, which in its turn lead to a reduced computational burden to solve the integral. For example, if 70% of the states sampled from $P(IWP)$ are clear sky states, and only 30% of those are included while sampling from $G(\mathbf{x})$ (i.e. $p_0 = 0.3$), the number of states in the retrieval will be decreased by $\sim 50\%$ compared to if the states were sampled from $P(IWP)$.

3.1.3 Measurement vector, noise and simulation uncertainty

The measurement vector to be used in the retrieval calculation should obviously contain the observed brightness temperature of the various ICI channels. Additional information, e.g. temperature and humidity information at difference pressure levels, available from ECMWF forecast model, can in principle also be added to the measurement vector.

However, it is preferable to let the measurement vector contain as few elements as possible, when applying the BMCI method. The reason for this is due to the fact that the states within the retrieval database must completely cover the measurement space. That is, there should be a number of states that "match" each possible measurement vector. Consequently, the required number of states that must be contained by the retrieval database increases with the dimension of the measurement vector.

The retrieval calculation can, by advantage, be performed in a "cloud signal space", by subtracting a reference clear sky measurement simulation from the measurement and simulated database states. That is, the measurement vector, to be used in the retrieval calculation for ICI, reads

$$y_j = \Delta \mathrm{Tb}_{o,j} = \mathrm{Tb}_{o,j} - F_{cs,j}(\mathbf{x}_o), \tag{3.5}$$

where $\mathrm{Tb}_{o,j}$ is the ICI observed brightness temperature of channel j and $F_{cs,j}(\mathbf{x}_o)$ is obtained from a clear sky (no hydrometeors) measurement calculation using ECMWF model data as input. A corresponding element of the database atmospheric state measurement vector reads

$$F_j(\mathbf{x}_i) = \Delta \mathrm{Tb}_{db,j,i} = F_{fs,j}(\mathbf{x}_i) - F_{cs,j}(\mathbf{x}_i), \tag{3.6}$$

where $F_{fs,j}(\mathbf{x}_i)$ and $F_{cs,j}(\mathbf{x}_i)$ are nominal and clear sky measurement simulations, respectively, for database state i and channel j. Any cloud properties of the $\mathbf{x}_i$ state are masked out in the $F_{cs,j}(\mathbf{x}_i)$ simulation.

The main advantage with this approach is that cloud information is compressed, since the contribution from the atmospheric background to the signal is decreased. When the effective dimension of the measurement vector is decreased, more states in the retrieval database tend to have a significant contribution to the integral (i.e. Eq. 3.2) for a given measurement.

The introduction of a clear sky measurement simulation in the state vector also comes with a risk of introducing a bias and adding noise in the retrieval due to incorporation of non-perfect data. The observed brightness temperatures of the ICI channels, for clear sky condition, primarily depends on atmospheric temperature and humidity (some channels have also significant surface sensitivity). To minimize the risk of introducing a bias, primarily only ECMWF temperature information will be used in the clear sky simulation, since the temperature is known to be very accurate. The relative humidity is set to a fixed value in the clear sky simulation (described in more detail in Sect. 3.4.1). The error of the clear sky simulation for channels with significant surface sensitivity is less critical for the ICI retrieval, since the retrieval will use information from such channels with caution (described in more detail in Sect. 3.4.1).

Knowledge of the measurement and simulation error covariance matrixes are required to solve Eq. 3.3. It is not straight forward to derive the full simulation error covariance matrix, and it also a computational demanding task to calculate the weight for each state i taking into account of the full observation error covariance matrix. If one assumes that the measurement

and simulation noise is uncorrelated between channels Eq. 3.3 can be described by

$$P(\mathbf{y}|\mathbf{x}_i) \sim exp\left(-\sum_{j=1}^{m}\frac{(y_j - F_j(\mathbf{x}_i))^2}{2\sigma_{e,j}^2}\right), \tag{3.7}$$

where the summation is performed over the m channels of ICI, and

$$\sigma_{e,j}^2 = \mathbf{S}_o(j,j) + \mathbf{S}_s(j,j) = \sigma_{o,j}^2 + \sigma_{s,j}^2 \tag{3.8}$$

is the system observation error (variance) for channel j. Eq. 3.7 is significantly less computational demanding to solve as compared to Eq. 3.3.

The measurement error ($\sigma_{o,j}$) has contributions both from NEΔT (see Table 2.1) of the measurement and from errors in the reference clear sky measurement simulation ($F_{cs,j}(\mathbf{x}_o)$). If one assume that the measurement simulation error is dominated by an imperfect modelling of the surface emissivity, the error can be approximated as

$$\sigma_{o,j}^2 \approx (\mathrm{NE}\Delta\mathrm{T}_j)^2 + (\Delta\varepsilon_j \mathrm{T}_{skin,j} e^{-\tau_j})^2, \tag{3.9}$$

where the second term of the right hand side represents an error due to non perfect modelled surface contribution, and T_{skin} is the surface temperature, τ_j and $\Delta\varepsilon_j$ is the atmospheric optical depth and error in surface emissivity for channel j, respectively. Thus, the surface contribution error is negligible if the atmospheric optical depth τ_j is high, but can otherwise be the dominating term of Eq. 3.9.

The database simulation error, $\sigma_{s,j}$, should be close to 0 for clear sky (or close to clear sky) states, while the error can be significant for states with high $\Delta\mathrm{Tb}_{db,j,i}$, due to both forward model errors and cloud parameter assumptions/simplifications. The magnitude of the simulation error mainly depends on how well the natural variability of cloud microphysics (i.e particle size distribution and particle habits) is incorporated in the retrieval database states. That is, the database simulation error can be used to compensate for the fact that it is, in practise, challenging to create a retrieval database that covers the full natural variability. For a given measurement with high $\Delta\mathrm{Tb}_{o,j}$ only database states having a similar cloud signal contribute to the integral (i.e. Eq. 3.2). Therefore $\sigma_{s,j}$, in practice, depends on $\Delta Tb_{o,j}$ and a simple parameterization reads

$$\sigma_{s,j}^2 \approx (c_j \Delta\mathrm{Tb}_{o,j})^2, \tag{3.10}$$

where c_j is a scale error factor for channel j. A realistic value of c (that takes into account the current microphysical variability of the ICI retrieval database), that is used for the ICI retrieval, is 0.03: the error (σ_s) in the simulation is 0.6 K, 1.2 K, and 3 K if $\Delta Tb_{o,j}$ is 20 K, 40 K, and 100 K, respectively.

A parameterisation of the system observation error (applied in the ICI retrieval algorithm) then reads

$$\sigma_{e,j}^2 \approx (\mathrm{NE}\Delta\mathrm{T}_j)^2 + (\Delta\varepsilon_j \mathrm{T}_{skin,j} e^{-\tau_j})^2 + (c\Delta\mathrm{Tb}_{o,j})^2. \tag{3.11}$$

This means that the system observation error is dominated by the NEΔT term if $\Delta\mathrm{Tb}_{o,j}$ is low and τ_j high, and by simulation error if $\Delta\mathrm{Tb}_{o,j}$ is high, and by surface contribution error if τ_j and $\Delta\mathrm{Tb}_{o,j}$ are low.

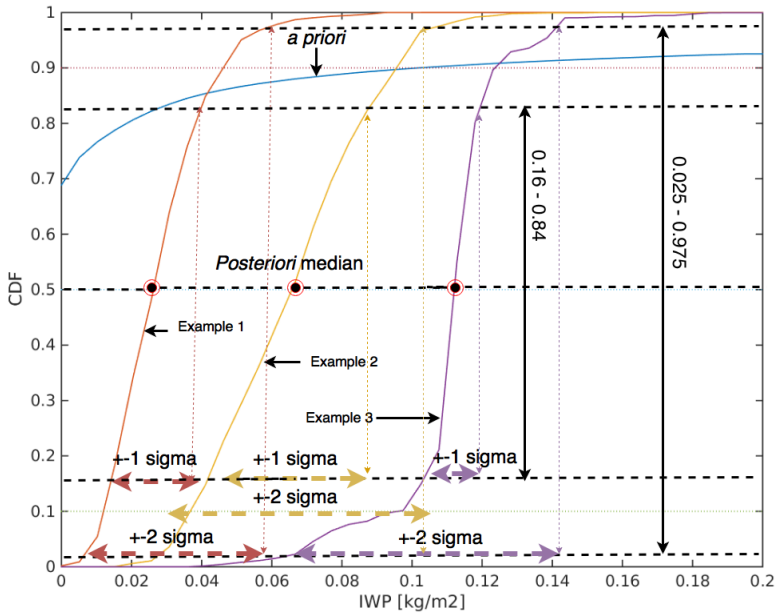

Figure 3.2: Example of IWP cumulative distribution functions (CDFs) and example error estimates. Blue line represents *a priori* CDF, and the other colored lines are three different examples of posterior CDFs.

3.1.4 Error estimates and posterior cumulative distribution

The BMCI calculation provides information that can be used to infer error estimates. The most general error estimate is a complete description of $P(\mathbf{x}|\mathbf{y})$ or the posterior cumulative distribution, $D(\mathbf{x}|\mathbf{y})$, and the relationship between the two can be described as

$$D(\mathbf{x}|\mathbf{y}) = \int_0^{\mathbf{x}} P(\theta|\mathbf{y})d\theta. \tag{3.12}$$

If $\mathbf{x}$ is a scalar (e.g IWP), $D(x|\mathbf{y})$ describes the probability ($[0-1]$) that x is smaller or equal to x given $\mathbf{y}$.

However, in practice it may be too ambitious to report the complete description of $P(\mathbf{x}|\mathbf{y})$ or $D(\mathbf{x}|\mathbf{y})$ as an error estimate for the ICI Level2 product. It is probably more suitable to report the IWP at some fixed values of $D(\mathbf{x}|\mathbf{y})$, for example the values that correspond to

- ± 1 standard deviations ($D(x_{-1\sigma}|\mathbf{y}) = 0.16$ and $D(x_{+1\sigma}|\mathbf{y}) = 0.84$), i.e there is a 68% probability that the true value of x is between $x_{-1\sigma}$ and $x_{+1\sigma}$
- ± 2 standard deviations ($D(x_{-2\sigma}|\mathbf{y}) = 0.025$ and $D(x_{+2\sigma}|\mathbf{y}) = 0.975$), i.e there is a 95% probability that the true value of x is between $x_{-2\sigma}$ and $x_{+2\sigma}$
- 5 and 95% confidence levels ($D(x_{min}|\mathbf{y}) = 0.05$ and $D(x_{max}|\mathbf{y}) = 0.95$) i.e there is a 95% probability that the true value of x is above x_{min} and a 95% probability that the true value of x is below x_{max}

Example CDFs and error estimates are displayed in Figure 3.2. A more detailed description of how the posterior CDF can be estimated at some fixed levels is described by meta code in Sect. 3.4.2.

3.2 Retrieval performance simulations and error sources

Figure 3.3 shows ICI retrieval performance simulation results for IWP, D_{mean}, and Z_{mean} (see Sect.2.2 for variable definitions and Sect.3.3 for assumptions/limitations relevant to the retrieval). The retrieval simulation was performed using one part of the ICI retrieval database (described in Sect. A.3) as a dataset of synthetic measurements with known underlying atmospheric states and the other part was used as a retrieval database by the retrieval algorithm (described in Sect.3.4). Both parts of the retrieval database contain simulations over both ocean and land. The retrieval algorithm outputs the ICI retrieval variables on levels of the posterior CDF. Figure 3.3 shows result for the 0.05, 0.5, and 0.95 levels (retrieval results have been binned and the median value of each level as function of the true value of the retrieval parameter is displayed). This means that the solid lines (0.5 CDF level) in Figure 3.3 can be seen as an averaged value of the "best estimate" of the retrieval algorithm, and the dashed lines as average estimates of the retrieval uncertainty. The lower and upper dashed lines have the meaning that there is a 95 % probability, that the value of the retrieval variable is above or below, respectively, this value.

The retrieval result is divided into three datasets (states with a surface temperature below 275 K, between 275 - 290 K, and above 290 K), in order to examine how ICI performs for various "meteorological regimes". The result is summarized in Table 3.1. The best retrieval performance is found for the warm surface temperature dataset for all three retrieval parameters. The average detection limit, or the IWP value at which one with a 95 % confidence can say that IWP is greater than 0 kg/m^2, is around 0.025 kg/m^2. The accuracy, or the difference between the retrieved posteriori median IWP and true IWP, is better than $\pm$50 % relative to the true IWP, for states with an IWP between 0.02 - 10 kg/m^2. The uncertainty, or the IWP values corresponding to the 5 and 95 % quantiles, is better than $\pm$50 % relative to the true IWP, for states with an IWP above 0.04 kg/m^2. D_{mean} is retrieved with an accuracy and uncertainty of approximately 20 μm and 50-100 μm, respectively. Z_{mean} is retrieved with an accuracy and uncertainty of approximately 500 m and 1000 m, respectively, for true Z_{mean} between 3 - 13 km.

The retrieval performance for the two datasets with lower surface temperatures are found to be significantly lower than that for the warm surface temperature dataset. The main error sources of the ICI retrieval, and how they are incorporated in the retrieval algorithm, are described in Table 3.2. The smoothing error (or the natural variability of cloud ice structures and how well these are measured by ICI) is particularly severe for the two colder surface temperature datasets. The main reason for this is due to the fact that the warm surface temperature dataset mainly consists of states where the cloud ice is located at least a few kilometer above the Earth's surface, whereas the lower surface temperature datasets contain a significant amount of states with cloud ice in the lowermost troposphere. Low altitude cloud ice is more complicated in the ICI retrieval primarily due to the fact that the signature in measured spectra is weaker for low altitude cloud ice mass (only a few of the lower frequency channels of ICI tend to have sensitivity to low altitude cloud ice mass) than for high altitude

cloud ice. Additionally, channels that have non negligible surface contribution are used with care by the retrieval algorithm (described in detail in Sect.3.4), since our ability to model the surface contribution is limited. Channels, for which the clear sky optical depth was lower than 1 and 3, for ocean and land pixels, respectively, were not used in the first iteration of the retrieval algorithm. This, further decreases the sensitivity to low altitude cloud ice mass, in particular over land. The effect of a low sensitivity to low altitude cloud ice is most clearly seen in the lower right panel of Figure 3.3, which shows that the retrieval performance is poor for $Z_{mean} \leq 3\,\mathrm{km}$, i.e. a low accuracy and high uncertainty (a bias towards apriori which is particularly strong for the coldest surface temperature dataset). A low sensitivity to low altitude cloud ice mass will not only be problematic for states that actually contain low cloud ice mass, it will also decrease the accuracy of all other retrieval parameters, as low altitude cloud ice mass is an integrated component of all of the ICI primary retrieval parameters.

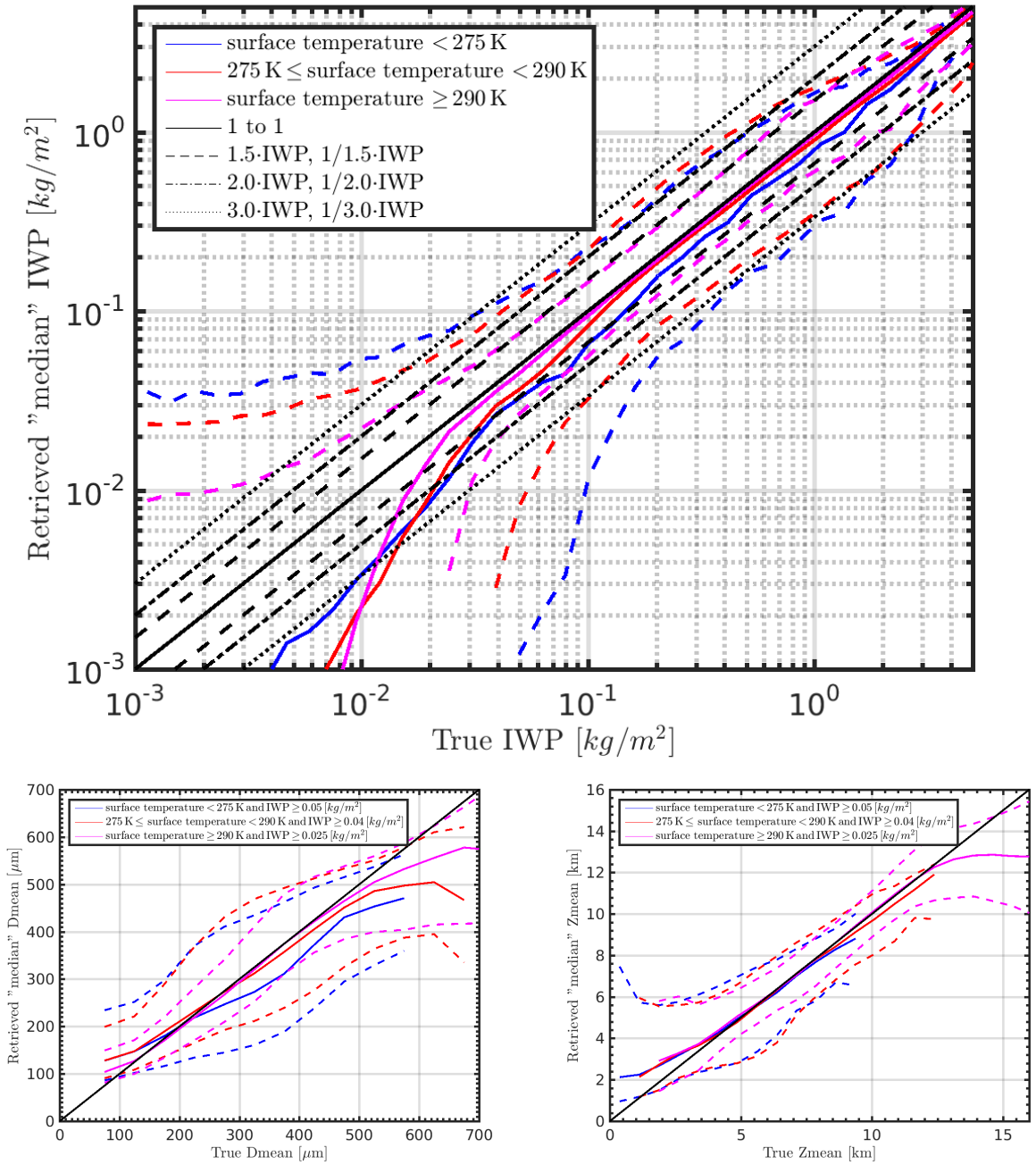

Figure 3.3: ICI retrieval performance simulation result for IWP (top panel), D_{mean} (lower left panel), and Z_{mean} (lower right panel). See text for more description.

Table 3.1: ICI retrieval performance summary.

Retrieval variable	Description
IWP	• surface temperature $\geq 290\,\mathrm{K}$ – the average IWP detection limit is around $0.025\,\mathrm{kg/m^2}$ (if we define the detection limit as the level where one with a 95 % probability can say that IWP is greater than $0\,\mathrm{kg/m^2}$). – The retrieval accuracy is better than ± 50 % for states with an IWP between 0.02 - $10\,\mathrm{kg/m^2}$. – The 5 - 95 % retrieval uncertainty is within the range (1/1.5·IWP, 1.5·IWP), for states with an IWP between 0.05 - $1.0\,\mathrm{kg/m^2}$. • $275\,\mathrm{K} \leq$ surface temperature $< 290\,\mathrm{K}$ – The IWP detection limit is around $0.04\,\mathrm{kg/m^2}$. – The 5 - 95 % retrieval uncertainty is within the range (1/3·IWP, 2·IWP) for states with an IWP between 0.1 - $1.0\,\mathrm{kg/m^2}$. • surface temperature $< 275\,\mathrm{K}$ – The IWP detection limit is around $0.05\,\mathrm{kg/m^2}$. – The 5 - 95 % retrieval uncertainty is within the range (1/3·IWP, 2·IWP) for states with an IWP between 0.4 - $1.0\,\mathrm{kg/m^2}$.

Continued on next page

Table 3.1 – continued from previous page

Source	Description
Z_{mean}	• surface temperature $\geq 290\,\mathrm{K}$ – The accuracy of the Z_{mean} retrieval is better $\pm 0.5\,\mathrm{km}$ for true Z_{mean} values between 3 - 13 km. – The 5 - 95 % retrieval uncertainty is approximately $\pm$ 1 km. • $275\,\mathrm{K} \leq$ surface temperature $< 290\,\mathrm{K}$ – The accuracy of the Z_{mean} retrieval is better $\pm 0.5\,\mathrm{km}$ for true Z_{mean} values between 3 - 12 km. – The 5 - 95 % retrieval uncertainty is approximately $\pm$1 - 2 km. • surface temperature $< 275\,\mathrm{K}$ – The accuracy of the Z_{mean} retrieval is better $\pm 0.5\,\mathrm{km}$ for true Z_{mean} values between 3 - 9 km. – The 5 - 95 % retrieval uncertainty is approximately $\pm$1 - 2 km.
D_{mean}	• surface temperature $\geq 290\,\mathrm{K}$ – The accuracy of the D_{mean} retrieval is within $\pm 20\,\mu$m for true D_{mean} values between 80 - 530 μm. – The 5 - 95 % retrieval uncertainty is approximately $\pm$ 50-100 μm. • $275\,\mathrm{K} \leq$ surface temperature $< 290\,\mathrm{K}$ – The accuracy of the D_{mean} retrieval is within $\pm 40\,\mu$m for true D_{mean} values between 100 - 500 μm. – The 5 - 95 % retrieval uncertainty is approximately $\pm$ 50-150 μm. • surface temperature $< 275\,\mathrm{K}$ – The accuracy of the D_{mean} retrieval is within $\pm 50\,\mu$m for true D_{mean} values between 100 - 500 μm. – The 5 - 95 % retrieval uncertainty is approximately $\pm$ 50-150 μm.

Table 3.2: Retrieval error sources.

Error source	Description
measurement noise	• the measurement noise (NEΔT, Table 2.1) give rise to a retrieval error, and is included as a component in the observation system noise (see Sect 3.1.3).
surface emissivity uncertainty	• imperfect forward modeling of surface emissivity introduces an error in the retrieval calculation. This error is modeled and included as a component of the observation system noise as described in Sect 3.1.3.
simulation error	• The simulation error is due to both forward model errors and applied cloud parameter assumptions/simplifications for generating the retrieval database. This error is modeled and included as a component of the observation system noise as described in Sect 3.1.3.
smoothing error	• The smoothing error is due to the fact that cloud structures and particle microphysical parameters can vary within the sampled volume of ICI, i.e on a vertical scale not resolved by ICI. The resulting retrieval uncertainty is captured by the retrieval algorithm in a statistical manner, as the retrieval output is a weighted average of database states. Each database state is having a realistic vertical varying cloud structure as the states are generated using cloud radar and lidar measurements as data source as described in Appendix. A.3.
beam filling error	• The beam filling error is due to the fact that cloud structures may vary on a horizontal scale within the ICI footprint, e.g only a part of the footprint may be covered by a cloud system. In practice, the resulting retrieval error can be captured by the ICI retrieval algorithm if the states in the retrieval database are created taking 3-dimensional effects into account. However, the current version of the ICI retrieval database, only captures a pseudo 2-dimensional variation of atmospheric state, as described in Appendix. A.3.

3.3 Assumptions and limitations

Main assumptions and limitations relevant to the ICI retrieval algorithm are:

- Only measurements from ICI will be used in the retrieval calculation.
- ICI has trough some of it's channels sensitivy to the lowest part of troposhere, and ocassionally also a high sensitivy to the Earth's surface. This is an important feature of ICI as it is important to be sensitive to low altitude cloud ice mass. However, it is just recently that a sea surface emissivity model for ocean covering the ICI channels has become available (Tool to Estimate Sea-Surface Emissivity from Microwaves to sub-Millimeter waves, TESSEM). Over land, their is no emissivity model available at the frequencies where ICI operates. This means that when ICI channels become sensitive to surface, their use is problematic and will therefore be used with caution. Effectively, this will introduce a retrieval error that can be severe for certain conditions, mainly for high latitude and low level clouds, as described in Sect. 3.2 and Appendix C.2.
- The retrieval algorithm is based on a retrieval database. In theory, the true PDF of atmospheric states should be known in order to create this database with correct statistical properties. This true PDF is extremely complex with respect to cloud properties and not perfectly known. Thus a number assumptions must be made in order to create this retrieval database, and these are described in more detailed in Appendix. A. The main assumption is probably with respect to cloud particle models (i.e. particle habit and size distribution). The required single scattering properties of complex shaped ice particles are presently only available for a limited number of particle types. It is assumed that the most important point is not to include all potential particle shapes, but to include a few types that covers the range of the scattering strength of natural occurring ice particle habits. The current retrieval database only contains randomly oriented particle types. This is an evident limitation as particles having a preferred orientation can give rise to polarisation effects. This is not only of concern for the 243.2 ± 2.5 GHz and 664.0 ± 4.2 GHz channels that measure both H and V polarisation, but also for all other channels that only measure V polarisation.

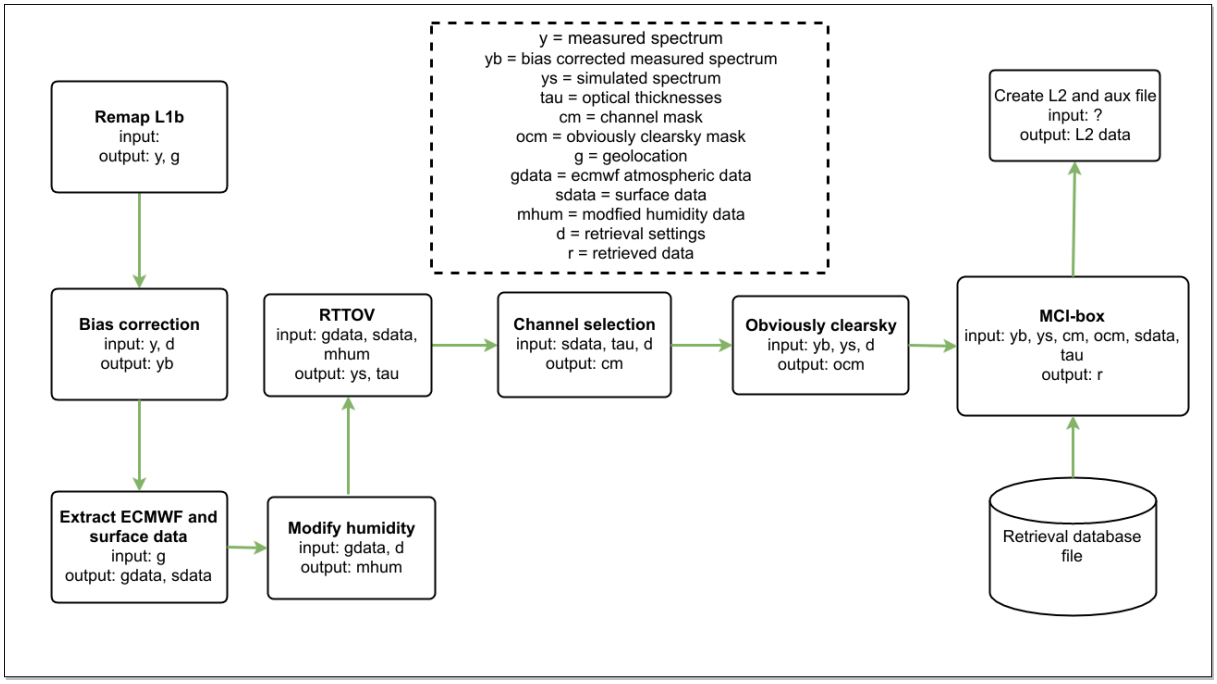

Figure 3.4: A graph describing the data flow in the proposed retrieval algorithm.

3.4 Retrieval processing chain

3.4.1 Overview of processing components and data flow

Figure 3.4 describes the data flow within the ICI Level2 processing chain. The actual retrieval calculation is performed within the "MCI-box", which is described in detail in Sect. 3.4.2. Boxes found to the left of the "MCI-box" can be seen as a preprocessing chain of the ICI retrieval algorithm. The aims of the preprocessing steps are:

- perform a bias correction, if necessary
- ingest atmospheric and surface data for the geolocation of the measurement in order to be able to:
  - identify which ICI channels that can safely be used in the retrieval calculation (i.e identify channels with negligible surface influence)
  - identify measurements that are obviously "clear-sky" observations (i.e measurements where one on beforehand, and with high probability, can guess that IWP is 0 [Kg/m^2]). This is not a necessary step, but to identify and exclude such measurements from further processing will save computation time
  - transform the observation to "cloud-signal" space
  - make an adequate selection of database states (see further Sect. 3.4.2)

A more detailed description of the various components of the processing chain is given below:

- **Remap L1B**: provides the processing chain with Level1B data. This module is only responsible for extracting relevant information from Level1B swath data to be used for further calculation.
  input: L1B swath data
  output: geolocation data: latitude, longitude, altitude, time, and footprint land fraction of the measurement, and angular relation for the earth view (satellite zenith and azimuth angles)
  measured spectrum: calibrated brightness temperature and radiometric noise of the ICI channels
  channel quality flags: status information of the various ICI channels (instrument and processing degradation).

- **Bias correction**: possibly applies a simple linear bias correction to the observed brightness temperatures, i.e

$$\mathrm{Tb}'_{o,j} = a_j + b_j \cdot \mathrm{Tb}_{o,j}. \tag{3.13}$$

  The main reason for why this module is included is that it is possible that there is an imperfect match (bias) between the statistics of observed and retrieval database state cloud signals, $\Delta\mathrm{Tb}_o$ and $\Delta\mathrm{Tb}_{db}$, e.g. due to that an imperfect absorption model was used in the simulation. If this is found the be the case, then this bias correction module can be used as a quick fix to the bias problem (modify Tb_o and thereby $\Delta\mathrm{Tb}_o$), although the long term solution would be to recalculate the retrieval database with more accurate input data.
  input: measured spectrum, model parameters (see entry *bias correction* in Table 3.3)
  output: bias corrected measured spectrum

- **Extract ECMWF and surface data**: extract ECMWF atmospheric (pressure, temperature, humidity) and surface (surface skin temperature, pressure, wind speed and direction, sea ice concentration, and snow depth) data, and surface altitude and type, for the geolocation of the measurement. The surface data (including footprint land fraction from Level1B data) are used to calculate basic surface type fraction and mask within the footprint, according to:

$$\text{surface type fraction} = \begin{cases} \textit{water faction:} \\ \quad (1 - \text{footprint land fraction}) \cdot (1 - \text{sea ice concentration}), \\ \textit{ice fraction:} \\ \quad (1 - \text{footprint land fraction}) \cdot \text{sea ice concentration}, \\ \textit{snow fraction:} \\ \quad \text{snow mask} \cdot \text{footprint land fraction} \\ \quad \text{where snow mask} = \text{snow depth} \geq \text{minimum snow depth}, \\ \textit{land fraction:} \\ \quad \text{footprint land fraction} \cdot (1 - \text{snow mask}), \end{cases} \tag{3.14}$$

and

$$\text{surface type mask} = \begin{cases} \textit{water} \text{ where:} \\ \quad \text{water fraction} \geq c_{min}, \\ \textit{ice} \text{ where:} \\ \quad \text{ice fraction} \geq c_{min}, \\ \textit{snow} \text{ where:} \\ \quad \text{snow fraction} \geq c_{min}, \\ \textit{land} \text{ where:} \\ \quad \text{land fraction} \geq c_{min}, \\ \textit{mixed} \text{ where:} \\ \quad \text{none of the above is valid,} \end{cases} \tag{3.15}$$

where c_{min} is a minimum fraction value (typically around 0.95).

The atmospheric and surface data will be used as input to simulate clear sky brightness temperatures and optical depths for the various ICI channels, and the surface mask will, additionally, be used within the "MCI-box".
input: geolocation data
output: atmospheric and surface data as described above

- **Modify humidity**?: modify the ECMWF tropospheric humidity profile, to be used in the clear sky simulation, to a fixed relative humidity (RH) value. Effectively, only ECMWF temperature data, but not humidity data, are used as *a priori* data for the ICI retrieval algorithm. The reason for this is that the ECMWF temperature data are more reliable than the humidity data. The tropospheric humidity profile is modified to a fixed RH w.r.t water value at pressure levels where the temperature is above 273.15 K, and to a fixed RH w.r.t. ice value at pressure levels where the temperature is below 253.15 K. A linear transition between RH w.r.t. water and ice, determined by temperature, is used between 273.15 K and 253.15 K. The applied parameterisation to calculate equilibrium pressure e_p for water and ice [Sonntag, 1994] can be described as:

$$e_p = \exp\left(\frac{c_1}{T} + c_2 + c_3 T + c_4 T^2 + c_5 \log(T)\right), \tag{3.16}$$

$$\text{where} \begin{cases} \text{water} & \text{ice} \\ c_1 = -6096.9385 & c_1 = -6024.5282 \\ c_2 = 21.2409642 & c_2 = 29.32707 \\ c_3 = -2.711193 \cdot 10^{-2} & c_3 = 1.0613868 \cdot 10^{-2} \\ c_4 = 1.673952 \cdot 10^{-5} & c_4 = -1.3198825 \cdot 10^{-5} \\ c_5 = 2.433502 & c_5 = -0.49382577 \end{cases},$$

and T is temperature in Kelvin. The modification described above is only applied to the tropospheric humidity profile. To avoid modify stratospheric values, no modifications is done if the original water vapor profile has a volume mixing ratio lower than 20 ppm.
input: atmospheric data, model parameter (see entry *modify humidity* in Table 3.3)

output: modified atmospheric humidity data

- **RTTOV**: simulate clear sky (no hydrometeors) brightness temperatures (Tb_{cs}) and optical thicknesses (τ_{cs}) for the ICI channels using the radiative transfer model RTTOV. Modelling of surface emissivities is of particular importance and for this purpose TESSEM (Tool to Estimate Sea Surface Emissivities in Microwave and Millimeter wave) and TELSEM (Tool to Estimate Land Surface Emissivities in Microwave and Millimeter wave) are deployed, with a possible modification as described below.

  It is more challenging to model surface emissivity over land, snow, and ice surfaces than over open water where the emissivity primarily is related to wind speed. Surface emissivities depends on many parameters for land, snow, and ice surfaces, and TELSEM is built around a satellite derived surface emissivity climatology with a 25[km] resolution. Inputs to TELSEM are latitude, longitude, month, incidence angle, and frequency and outputs are emissivities (at V and H polarization). A direct use of TELSEM, for this application, can result in significant errors, for example if the footprint is actually only partly covered by sea ice but completely covered according to the TELSEM climatology. Additionally, surface emissivity modelling in coastal regions can also lead to errors, as the TELSEM climatology has a lower resolution than the ICI footprints (a footprint weighted surface emissivity in coastal region is a mixture between land and water emissivity).

  A potential solution to the described problem is to give a special treatment to the small fraction of pixels with an associated mixed surface type (see Eq. 3.15). Separate simulations can be performed for each surface type involved and obtained brightness temperatures are weighted according to the footprint surface type fraction (see Eq. 3.14). However, the implementation of this solution requires a non-direct use of TELSEM or some other alternative (to be decided).

  Simulated brightness temperatures and optical thicknesses will be used for two different purposes. The simulated τ_{cs} will be used by the channel selection module. The simulated Tb_{cs} will be used by the actual retrieval calculation, which is performed in the cloud signal space ($\Delta\mathrm{Tb}_o = \mathrm{Tb}_o - \mathrm{Tb}_{cs}$).
  input: (modified) atmospheric and surface data
  output: simulated clear sky brightness temperatures and optical thicknesses for the ICI channels

- **Channel selection**: performs a first channel selection; only channels that have an acceptable quality according to the Level1b data will be used for further calculation. Additionally, only channels that have a limited sensitivity to the surface will be selected for further use, in order to not introduce a retrieval error due to an imperfect modelling of surface contribution to the measurement. The selection is based on simulated τ_{cs} and on defined optical depth threshold values. Different threshold values ($\tau_{min,water}$, $\tau_{min,ice}$, $\tau_{min,snow}$, $\tau_{min,mixed}$, and $\tau_{min,land}$) are defined and applied according to the surface type mask (Eq. 3.15). The reason for the discremenation between surface types is due to the

fact that the errors in the surface emissivity modelling (see *RTTOV*) depends on surface type. A channel with significant surface influence will not be used in the retrieval calculation, i.e.

$$\text{channel is not ok to use if } \begin{cases} \tau_{cs} \leq \tau_{min,water} \text{ for water surface footprints,} \\ \tau_{cs} \leq \tau_{min,ice} \text{ for ice surface footprints,} \\ \tau_{cs} \leq \tau_{min,snow} \text{ for snow surface footprints,} \\ \tau_{cs} \leq \tau_{min,mixed} \text{ for mixed surface footprints,} \\ \tau_{cs} \leq \tau_{min,land} \text{ for land surface footprints,} \end{cases} \tag{3.17}$$

where the values of the $\tau_{min,water}$, $\tau_{min,ice}$, $\tau_{min,snow}$ $\tau_{min,mixed}$, and $\tau_{min,land}$ are intented to be set in such a way that resulting error in the clear sky simulation, due to imperfect surface modelling, will be smaller than ~ 0.5K, for the channel to be used.

A consequencue of our limited ability to model surface contribution and having a lower threshold value for open water than for other surfaces is clearly that it is possible that the quality of the ICI retrieval for low altitude cloud ice is better over water than other surfaces, due to the fact that more channels may be used in the retrieval. However, the τ_{min} parameters can be updated when our ability to model surface contribution increases.
input: channel quality flag, surface type mask, simulated clear sky optical thicknesses, model parameters (see entry *channel selection* in Table 3.3)
output: channel selection mask

- **Obviously clearsky**: the module aims to identify measurements taken at dry atmospheric conditions and that can be classified as "obviously clearsky". The underlying objective of the module is to allow for a reduction of computation time, as no IWP retrieval calculation is necessary for those measurements. Approximately 70% of all ICI pixels may be cloud free, but all of them can certainly not be classified as "obviously clearsky". Simulation test revealed that about 40 % of the ICI observations will be classified as obviously clearsky by applying the algorithm as described below. This implies that computation time can be decreased by almost 40 %.

  If the atmosphere is dry the "cloud signal" or $\Delta\text{Tb}_{o,j}$ tends to be positive and high, and the clearsky test is therefore done by examine if

$$\Delta\text{Tb}_{o,j} \geq \Delta T_j, \tag{3.18}$$

  where ΔT_j is a threshold value for channel j and a suitable value of ΔT_j was found to be $3 \cdot \text{NE}\Delta\text{T}_j$ (see Figure 3.5). The test is executed for some selected ICI channels. The ICI channels are grouped into five group of channels, where each group of channels shares a

common radiometer, i.e

$$\text{group of channels} = \begin{cases} \text{group 1:} \\ \quad \text{ICI-1}\,(183.31 \pm 7.0\,\text{GHz}) \\ \quad \text{ICI-2}\,(183.31 \pm 3.4\,\text{GHz}) \\ \quad \text{ICI-3}\,(183.31 \pm 2.0\,\text{GHz}) \\ \text{group 2:} \\ \quad \text{ICI-4}\,(243.2 \pm 2.5\,\text{GHz}) \\ \text{group 3:} \\ \quad \text{ICI-5}\,(325.15 \pm 9.5\,\text{GHz}) \\ \quad \text{ICI-6}\,(325.15 \pm 3.5\,\text{GHz}) \\ \quad \text{ICI-7}\,(325.15 \pm 1.5\,\text{GHz}) \\ \text{group 4:} \\ \quad \text{ICI-8}\,(448.0 \pm 7.2\,\text{GHz}) \\ \quad \text{ICI-9}\,(448.0 \pm 3.0\,\text{GHz}) \\ \quad \text{ICI-10}\,(448.0 \pm 1.4\,\text{GHz}) \\ \text{group 5:} \\ \quad \text{ICI-11}\,(664.0 \pm 4.2\,\text{GHz}) \end{cases} \tag{3.19}$$

Each group of channels is considered to be equally important for the clear sky test, but the definition of group of channels above also describes the priority order of the channels from within a given group. For example, if all channels are allowed to be used, according to the "Channel selection" algorithm, ICI-1, ICI-4, ICI-5, ICI-8, and ICI-11 will be used by the "Obviously clearsky" algorithm in order to decide if a measurement is "obviously clearsky".
input: channel selection mask, simulated clear sky brightness temperatures, measurement spectrum, model parameters (see entry *obviously clearsky* in Table 3.3)
output: obviously clear sky mask

- **MCI − box**: performs the actual retrieval calculation (described in Sect. 3.4.2).

- **Create L2 and aux file**: creates the output level2 file
  input: measurement spectrum, channel quality mask, simulated clear sky brightness temperatures and optical thicknesses, geolocation data, channel selection mask, obviously clear sky mask, retrieval data
  output: output level2 file (see Sect. 3.6)

- **retrieval database file**: a database file consisting of synthetic atmospheric states and corresponding simulated measurements, to be used by **MCI − box**. See Appendix A.5 for anticipated database file format and content.

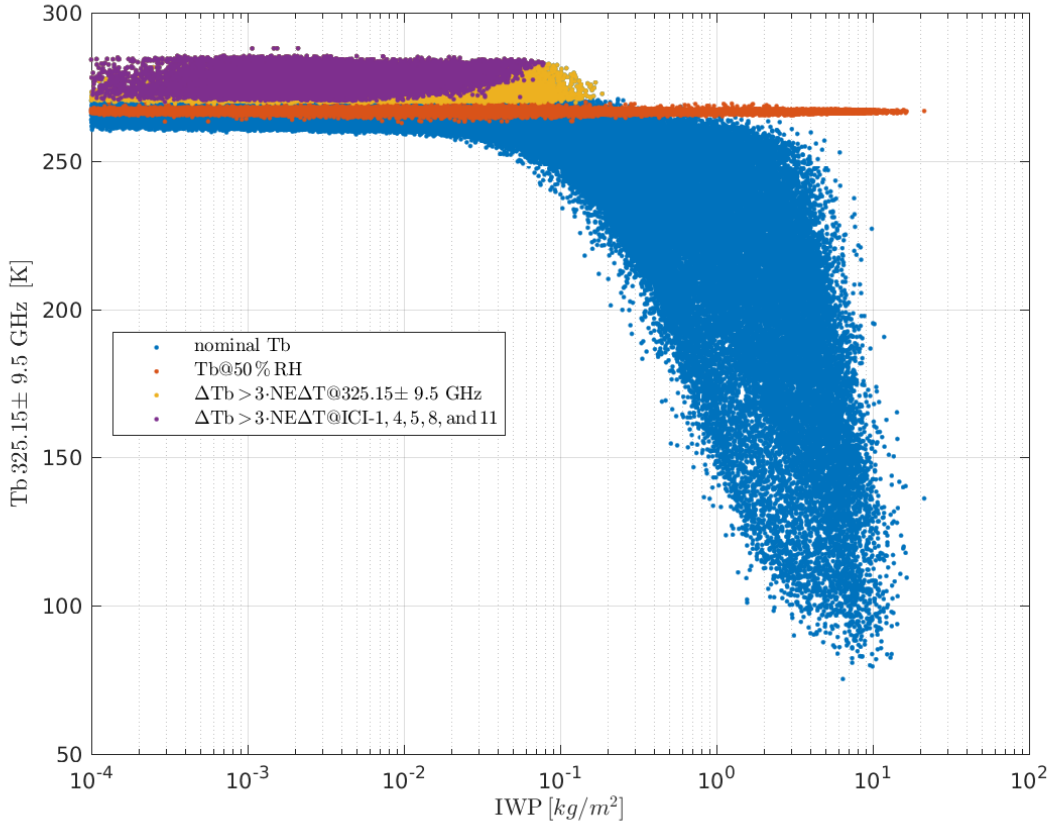

Figure 3.5: Schematic of the obvioulsy clearsky algorithm. The blue dots show simulated brightness temperatures (Tb) at 325 ± 9.5 GHz as function of IWP for varying atmospheric conditions. The brownish dots show simulated clear sky (no hydrometeors) brightness temperatures (Tb_{cs}) for the same atmospheric states as the blue dots, but the tropospheric humidity profile of each state has been modified and set to 50 % RH (according the **Modify humidity**? algorithm). The yellow dots are overlaid on top of blue dots that have a cloud signal $\Delta Tb = Tb - Tb_{cs} \geq 3 \cdot NE\Delta T$ at 325 ± 9.5 GHz. The purple dots are overlaid on yellow and blue dots where $\Delta Tb \geq 3 \cdot NE\Delta T$ for channel 1, 4, 5, 8, and 11 of ICI (i.e the purple points will be classified as clearsky states by the **Obviously clearsky** algorithm, with the meaning that the cloud signature is s weak in these "observations" so it is no point in making a retrieval because we already know that we will retrieve a 0 IWP for these states).

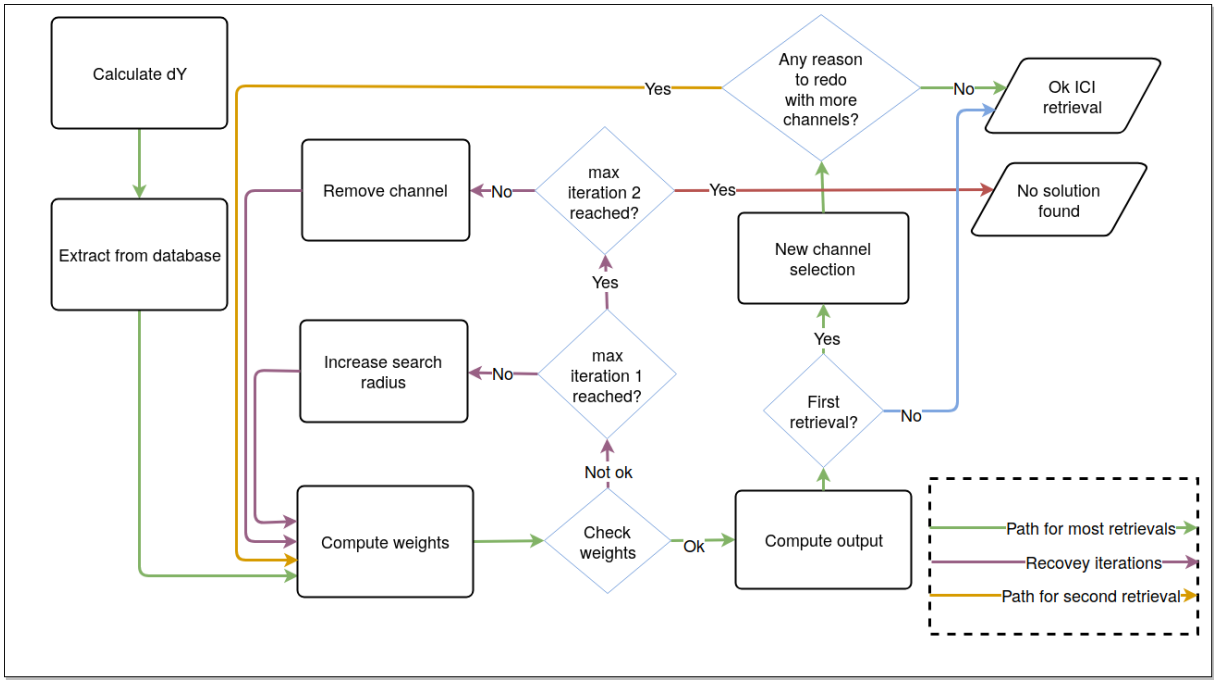

Figure 3.6: A graph describing the "MCI-box", i.e. the core of the retrieval algorithm. An iterative algorithm is applied to ensure that a retrieval solution can be found for all measurements, although most retrievals are anticipated to be succesfully calculated with no iteration. A second retrieval is possibly done for observations that are heavily influenced by clouds.

3.4.2 Monte Carlo integration scheme for ICI

Figure 3.6 shows an overview of the MCI scheme (MCI-box) applied for ICI. The MCI-box contains a number of sub-modules that is described in more detail below, but first a high level overview is given.

MCI – box

input: measurement spectrum, channel quality mask, simulated clear sky brightness temperatures and optical thicknesses, geolocation data, channel selection mask, obviously clear sky mask, retrieval database, model parameters (see Table 3.4)

output: retrieved IWP, D_{mean}, and Z_{mean} including error estimates, retrieval quality flags: status, number of database hits, number of channels used in retrieval, parameters describing the final iteration state of retrieval i.e number of iterations for "increasing search radius", "remove channel", and "any reason to redo with more channels?"

optional: retrieved liquid water path, total column water vapor, rain water path, and cloud ice habit probability

The retrieval algorithm effectively interpolates between states in a retrieval database that match the observation. More specifically, weights are calculated for database states depending on how close the match is, and from these weights best estimates and uncertainties of retrieval variables can be derived. Ideally, the retrieval database should be large enough and represent reality in such a way that there for each possible measurement is a high number of states that

match the measurement. In reality it is difficult to construct a retrieval database that fulfills this criteria.

The aim of the retrieval algorithm is therefore to make best possible use of the information of the observation, and handle the situation when the match between an observation and all states in the retrival database is poor. An iterative algorithm is applied to ensure that a retrieval solution can be found for all meassurements. However, the retrieval calculation is anticipated to follow the green arrows in Fig. 3.6 for most observations (i.e. no iteration), and by using information from selected ICI channels as described in Sect. 3.4.

The iterative scheme applied (see purple arrows in Fig. 3.6) can be divided into two types of iterations. If it is found that too few database states match the observation, the criteria for what is considered to be a valid match is first relaxed. If the number of matches is still low, the algorithm will screen out ICI channels in the retrieval calculation. Both of these actions can be seen as a recovery solution to the underlying problem that the retrieval database does not cover the measurement space satisfactory. It is anyhow judged that it is better if the retrieval algorithm produce an output with a high uncertainty than to produce no output at all.

The retrieval calculation is possibly repeated (a maximum of one time) if the observation is found to be heavily influenced by clouds (see yellow arrow in Fig. 3.6). A second retrieval is then executed if it is judged that information from additional ICI channels can safely be used (negliable surface influence beacause cloud optical depth is high) in the calculation.

- **Calculate dy**: calculate the cloud signal

$$y_j = \Delta \mathrm{Tb}_{o,j} = \mathrm{Tb}'_{o,j} - \mathrm{Tb}_{cs,j} \tag{3.20}$$

  of the observation and estimate system observation noise $\sigma_{e,j}$ (Eq. 3.10). The retrieval calculation is performed in cloud signal space, as explained in Sect. 3.1.3.
  input: (bias corrected) measured spectrum, simulated clear sky spectrum and optical thicknesses, model parameters (see entry *calculate dy* in Table 3.4)
  output: cloud signal, observation system noise

- **Extract from "database"**: fetch states from the database that match the measurement to be inverted. The main aims of this module are to:

  1. select states where the cloud signal is more or less consistent to the observation. This is important for a computational efficiency reason. States with a poor match will and should not have an impact on the retrieval (apart from adding a significant computational cost for other modules) and can therefore be excluded.
  2. select states with smiliar meteorological conditions as of the geolocation of the observation (i.e surface pressure, surface temperature, surface wind speed, and surface type). This is important for a physical reason, since the selected database states will be used as a priori data, and Appendix B describes the importance of using surface parameter information in the retrieval calculation.
  3. select a sufficient number of states, which is of importance since we always want to be able to provide a retrieval result.

The retrieval database clearly does not contain states that exactly match a given measurements, hence an acceptable devation must be defined for each parameter used for the filtering. This can potentially results in that no or too few (for later calculations) states will be fetched, if acceptable deviations are small. This is clearly not desirable, and therefore the extraction procedure is done in an iterative manner, by increasing the search intervall by a factor of $\sqrt{2}$ in each iteration, until a sufficient number of database states has been selected. The filter used to fetch matching database states is described by:

$$\text{state } i \text{ matches if } \begin{cases} \Delta\text{Tb}_{o,j_1} - \sqrt{2}^k \cdot s \cdot \sigma_{e,j_1} \leq \Delta\text{Tb}_{i,j_1} \leq \Delta\text{Tb}_{o,j_1} + \sqrt{2}^k \cdot s \cdot \sigma_{e,j_1} \\ \ldots \\ \Delta\text{Tb}_{o,j_n} - \sqrt{2}^k \cdot s \cdot \sigma_{e,j_n} \leq \Delta\text{Tb}_{i,j_n} \leq \Delta\text{Tb}_{o,j_n} + \sqrt{2}^k \cdot s \cdot \sigma_{e,j_n} \\ \text{stm}_i = \text{f}(\text{stm}_o) \\ \text{st}_o \text{ - } \sqrt{2}^k \cdot \Delta\text{st} \leq \text{st}_i \leq \text{st}_o + \sqrt{2}^k \cdot \Delta\text{st} \\ \text{sw}_o \text{ - } \sqrt{2}^k \cdot \Delta\text{sw}(\text{stm}_o) \leq \text{sw}_i \leq \text{sw}_o + \sqrt{2}^k \cdot \Delta\text{sw}(\text{stm}_o) \\ \text{sp}_o \text{ - } \Delta sp^{\sqrt{2}^k} \leq \text{sp}_i \leq \text{sp}_o + \Delta sw^{\sqrt{2}^k} \end{cases}$$

where

- $\Delta\text{Tb}_{o,j_1}$: cloud signal of observation for channel j_1 etc.
- $\Delta\text{Tb}_{i,j_1}$: cloud signal of database state i for channel j_1 etc.
- σ_{e,j_1}: system observation noise for channel j_1
- s: is a relative "search radius"
- k: denotes an iteration counter starting from 0

- stm_o: surface type mask at observation geolocation [-]
- stm_i: surface type mask for database state i [-]
- f(stm_o): a function that describes acceptable surface types for the observation [-], e.g.
  - f(water) = water
  - f(ice) = [ice, snow]
  - f(snow) = [ice, snow]
  - f(mixed) = [ice, snow, mixed, land]
  - f(land) = land

- st_o: surface temperature at observation geolocation [K]
- st_i: surface temperature for database state i [K]
- Δst: surface temperature acceptable deviation [K]

- sw_o: surface wind speed at observation geolocation [m/s]
- sw_i: surface wind speed for database state i [m/s]
- $\Delta\text{sw}(\text{lsm}_o)$: a land sea mask dependent wind speed acceptable deviation [m/s]

- sp_o: surface pressure at observation geolocation [hPa]
- sp_i: surface pressure for database state i [hPa]
- Δsp: surface pressure acceptable deviation [hPa]

(3.21)

The test to check if database states are consistent to a given measurement uses observed

cloud signals from a limited number of channels. It is anticipated that all available channels (excluding channels with a high surface sensitivity) will be used in further step in the retrieval calculation for the majority of all pixels. However, only a limited number of channels are used for the selection of database states, since the retrieval algorithm contains a "recovery iteration" procedure where channels can be removed (in a defined order) from the retrieval calculation. This gives that it is not desirable to exclude states, for further calculations, based on low agreement of cloud signals from channels that have low priority, in the case that these channels will be excluded from the calculation (within the "remove channel" part of the algorithm). A channel priority defintion structure ("groups of channels") for the "extract from database" module is defined below:

$$\text{groups of channels} = \begin{cases} \text{group 1:} \\ \quad \text{ICI-1}\,(183.31 \pm 7.0[\text{GHz}]) \\ \quad \text{ICI-2}\,(183.31 \pm 3.4[\text{GHz}]) \\ \quad \text{ICI-3}\,(183.31 \pm 2.0[\text{GHz}]) \\ \quad \text{ICI-11}\,(664.0 \pm 4.2[\text{GHz}]) \\ \text{group 2:} \\ \quad \text{ICI-4}\,(243.2 \pm 2.5[\text{GHz}]) \\ \text{group 3:} \\ \quad \text{ICI-5}\,(325.15 \pm 9.5[\text{GHz}]) \\ \quad \text{ICI-6}\,(325.15 \pm 3.5[\text{GHz}]) \\ \quad \text{ICI-7}\,(325.15 \pm 1.5[\text{GHz}]) \\ \quad \text{ICI-8}\,(448.0 \pm 7.2[\text{GHz}]) \\ \quad \text{ICI-9}\,(448.0 \pm 3.0[\text{GHz}]) \\ \quad \text{ICI-10}\,(448.0 \pm 1.4[\text{GHz}]) \end{cases} \tag{3.22}$$

That is, three groups of channels are defined, and a maximum of one channel per group will be used by "extract from database". The ordering within each group depends on atmospheric opacity. ICI-1, ICI-4, and ICI-5 are associated with the lowest atmospheric opacity in each group, respectively, and these channels will preferably be used by "extract from database". The reasoning for ordering the channels according to atmospheric opacity is related to the experience that a single channel IWP retrieval performance is better for a channel that is sensitive to as large volume as posssible of the atmosphere.
input: geolocation data, cloud signal, observation system noise, channel selection mask, model parameters (see entry *extract from database* in Table 3.4)
output: database file data: simulated measurements and corresponding underlying state IWP, Z_{mean} D_{mean}, and optical thicknesses, and *a priori* weights.

- **Compute weights**: calculate weights (apply Eq. 3.7) for the selected database states.
  input: measured cloud signal, database cloud signals, observation system noise
  output: weights for the database states

- **Check weights**: checks that there is a sufficient number of database states that is consistent to the measurement. The expectation value and standard deviation of χ^2 for a perfect match between an observation and a database state (i.e. difference is only due to normal distributed noise) is

$$\mathbf{E}(\chi^2) = \mathbf{E}\left(\sum_{j=1}^{n}\left(\frac{\Delta\mathrm{Tb}_{o,j} - \Delta\mathrm{Tb}_{s,j}}{\sigma_{e,j}}\right)^2\right) = n \pm \sqrt{2n}, \tag{3.23}$$

where n is the number of channels. A database state is considered to be consistent to the measurement if the associated weight (w_i)

$$\begin{aligned} w_i &= a_i \exp\left(-\sum_{j=1}^{n}\left(\frac{\Delta\mathrm{Tb}_{o,j} - \Delta\mathrm{Tb}_{s,j}}{\sqrt{2}\sigma_{e,j}}\right)^2\right) \\ &\geq \exp\left(-\frac{n + s\cdot\sqrt{2n}}{2}\right), \end{aligned} \tag{3.24}$$

where a_i is an *a priori* weight and s is a scalar search radius. If the number of database states (n_{db-hit}) that match the observation, according to Eq. 3.24, is sufficiently large (greater than n_{min}), i.e

$$n_{db-hit} \geq n_{min}, \tag{3.25}$$

the retrieval calculation can proceed to "compute output". However, the subset of matching database states will be reduced in size, if the number of database hits is larger than required (greater than n_{max}), due to a computational efficiency reason. This is done by a random selection of states from this subset. A "recovery iteration" loop is exceuted (See Fig. 3.6), if the number of database hits is smaller than n_{min}.
input: weights, model parameters (see entry *check weights* in Table 3.4)
output: a flag indicating if $n_{db-hit} \geq n_{min}$

- **Increase search radius**: effectively, in this iteration step the limit of what is considered to be a measurement / database match is relaxed. In practice, the system observation noise levels of the considered ICI channels are synthetically increased, i.e

$$\sigma_{e,j}^{'} = c_j \cdot \sigma_{e,j}, \tag{3.26}$$

where c_j is a scale factor for channel j, and a new weight calculation will be performed, and each state will obtain a new and different weight than before. This step can be repeated *D.retrieval.max_iter* times when still at least one more channel can be removed, otherwise the iteration will continue.
input: model parameters (see entry *increase search radius* in Table 3.4)
output: updated $\sigma_e(j)$ values for the ICI channels

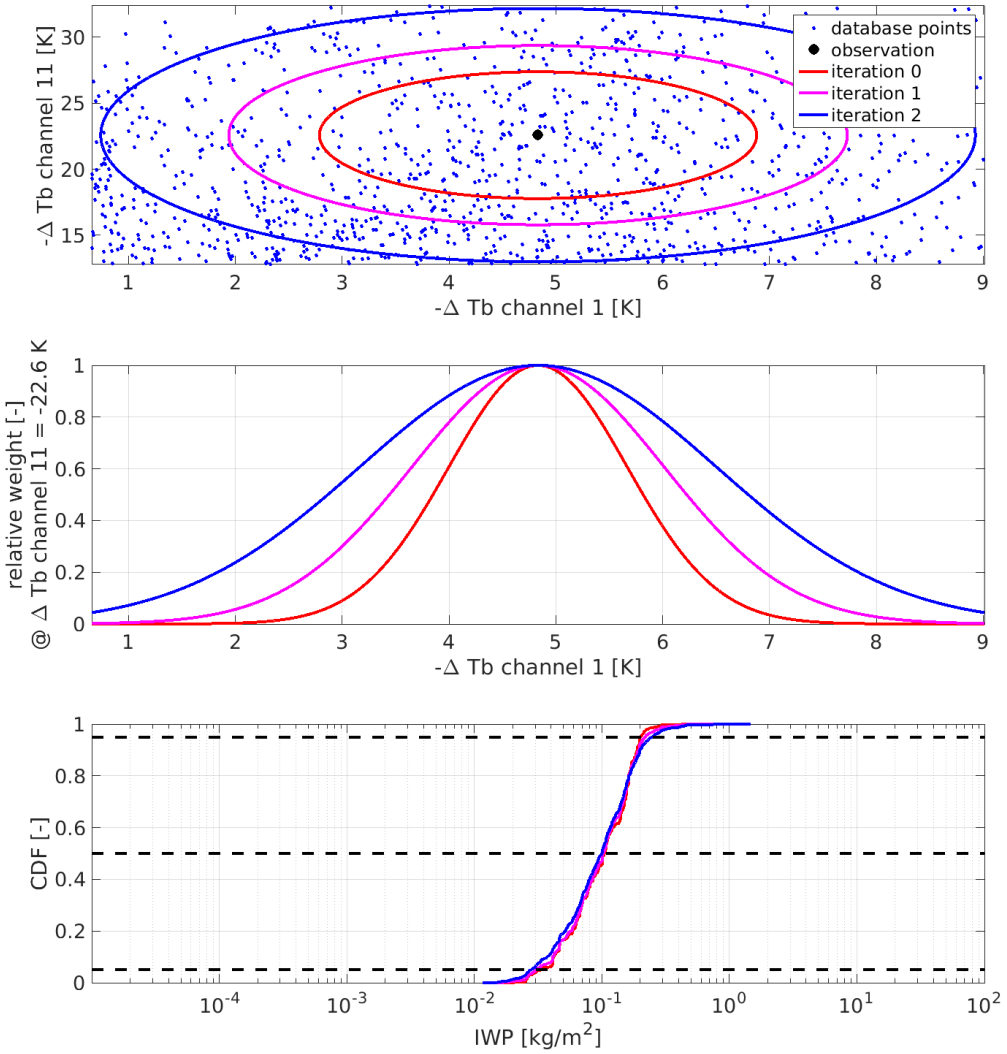

Figure 3.7: A schematic of increase search radius iteration. Upper panel shows a scatterplot of cloud signals from an observation and database states, in a 2-dimensional measurement space (channel 1 and 11). Additionally, ellipses of *check weights* threshold levels (Eq. 3.24) for an initial, first, and second iteration, are shown. The second panel shows relative weights (for a perfect channel 11 match) for an initial, first, and second iteration. The lower panel shows obtained posterior cumulatitive distribution functions for an initial, first, and second iteration.

- **Remove channel**: in this iteration step one ICI channel is removed from the retrieval calculation, according to a channel priority list, e.g.

$$\text{remove channel list} = \begin{cases} \text{ICI-10}\,(448.0 \pm 1.4[\text{GHz}]) \\ \text{ICI-9}\,(448.0 \pm 3.0[\text{GHz}]) \\ \text{ICI-8}\,(448.0 \pm 7.2[\text{GHz}]) \\ \text{ICI-11}\,(664.0 \pm 4.2[\text{GHz}]) \\ \text{ICI-7}\,(325.15 \pm 1.5[\text{GHz}]) \\ \text{ICI-3}\,(183.31 \pm 2.0[\text{GHz}]) \\ \text{ICI-6}\,(325.15 \pm 3.5[\text{GHz}]) \\ \text{ICI-2}\,(183.31 \pm 3.4[\text{GHz}]) \\ \text{ICI-5}\,(325.15 \pm 9.5[\text{GHz}]) \\ \text{ICI-1}\,(183.31 \pm 7.0[\text{GHz}]) \\ \text{ICI-4}\,(243.2 \pm 2.5[\text{GHz}]) \end{cases} \tag{3.27}$$

  where the first channel (ICI-10) will be removed first, and so on (the *remove channel list* ordering depends on atmospheric opacity following the same argument as described in *Extract from "database"* section). The channel removal is only done if the "Increase search radius" iteration did not help to find enough database matches. The rational for screening out a channel is that the likelihood of finding database matches will increase with a decreasing number of ICI channels considered. Anyhow, screening out a channel must be considered as a "recovery solution", since it means that the database coverage is limited and not sufficient, given that the ICI measurement is calibrated correctly. The iteration can be repeated until n number ICI channels remain.
  input: channel mask, model parameters (see entry *remove channel* in Table 3.4)
  output: updated channel mask

- **Compute output**: computes the retrieval output, i.e the *posterior* median values (and error estimates) of IWP, D_{mean}, Z_{mean}, and optical thicknesses (to be used by new channel selection). The retrieval is calculated individually for each parameter, and the median value of IWP and cloud optical thicknesses for the various channels are obtained as

$$x_{median} : D(x|\mathbf{y}) = 0.5, \tag{3.28}$$

  and the D_{mean} and Z_{mean} are obtained as

$$x_{median} : D(x|\mathbf{y}\,\&\,IWP > 0) = 0.5. \tag{3.29}$$

  That is, the retrieval of D_{mean} and Z_{mean} is calculated using the additional condition that IWP is greater than 0. The reason for this is that these parameters are properties of the state that are not defined if IWP = 0 (for example: what is the cloud height of a non existing cloud?). Suitable error estimates are the corresponding ± 1 (0.16 and 0.84) standard deviation levels, 0.05 and 0.95 levels, of the *posterior* cumulative distribution function.

A description how the median (and error estimate) values can be obtained in practice is given below using meta code:
A given database state is associated with a state vector
($\mathbf{x}_i = [IWP_i, D_{mean,i}, Z_{mean,i}, \tau_{1,i}, ..., \tau_{m,i}]$) and a scalar weight ($p_i$). If we denote the vectors (of length n) of weights for the considered database states by $\mathbf{p}$, the underlying retrieval variable (e.g IWP) by $\mathbf{x_{IWP}}$, and a discrete representation of the function $D(x|y)$ by $\mathbf{d}$ then:

For IWP (and for optical thicknesses):
$\mathbf{indexes} = sort(\mathbf{x}_{IWP})$
$\mathbf{x}_{IWP,sorted} = \mathbf{x}_{IWP}(\mathbf{indexes})$
$\mathbf{p}_{IWP,sorted} = \mathbf{p}(\mathbf{indexes})$
$\mathbf{d}_{IWP}(k) = \sum_{i=1}^{k} \mathbf{p}_{IWP,sorted}(i) / \sum_{i=1}^{n} \mathbf{p}_{IWP,sorted}(i)$
$cdf_{levels} = [0.05, 0.16, 0.5, 0.84, 0.95]$
$\mathbf{x}_{IWP,output} = interp(\mathbf{d}_{IWP,sorted}, \mathbf{x}_{IWP,sorted}, cdf_{levels})$

For D_{mean} (and Z_{mean}):
$\mathbf{indexes} = sort(\mathbf{x}_{D_{mean}})$ for indexes where IWP > 0
and then the remaining is equivalent as above.

A cloud particle model (Table A.1) probability can be estimated from the relative fraction of weight that is given to each cloud particle model type.

input: weights, IWP, Z_{mean} D_{mean}, and optical thicknesses, model parameters (see entry *compute output* in Table 3.4)
output: retrieved IWP, Z_{mean} D_{mean}, and optical thicknesses

- **Any reason to redo with more channels / New channel selection**: selection of a new set of channels that will be considered for a repeated retrieval calculation. Channels that have a significant surface influence, for clear sky conditions (i.e. an error in the clear sky simulation due to imperfect surface emissivity modelling of more than $\sim$ 0.5K), are excluded in the first retrieval calculation. In the case that retrieved cloud optical depths are high for channels that were excluded, a second retrieval may be considered, taking these channels into account. The reason for this is that the relative importance of the surface emissivity error will be less severe for an observation that is heavily influenced by cloud, due to both the fact that the total atmospheric optical depth is greater than the clear sky part and that cloud modelling error tends to dominate the observation system noise (see e.g Eq. 3.10). Thus, the retrieval accuracy should be better by including more channels, and an ICI channel will be re-selected if the weighted sum of clearsky optical depth and retrieved cloud optical depth is greater than a defined threshold level, accoding

to:

$$\text{channel } i \text{ is ok to use if } \begin{cases} \tau_{cs} + c \cdot \tau_{cloud,med} \geq \tau_{min,water} \text{ for water surface pixel} \\ \tau_{cs} + c \cdot \tau_{cloud,med} \geq \tau_{min,ice} \text{ for ice surface pixel} \\ \tau_{cs} + c \cdot \tau_{cloud,med} \geq \tau_{min,snow} \text{ for snow surface pixel} \\ \tau_{cs} + c \cdot \tau_{cloud,med} \geq \tau_{min,mixed} \text{ for mixed surface pixel} \\ \tau_{cs} + c \cdot \tau_{cloud,med} \geq \tau_{min,land} \text{ for land surface pixel} \end{cases} \tag{3.30}$$

where e.g. $\tau_{min,water}$ and $\tau_{min,land}$ are optical depth threshold levels for water and land pixels (parameters are shared with the "channel selection" module), and c is a scalar factor (with an intended value typically between 5 - 10) introduced due to the fact that τ_{cs} and $\tau_{cloud,med}$ impact the system observation noise in different ways, and are not directly comparable. The re-selction does not exclude any channel that was included in the first retrieval, even if the retrieved cloud optical depth is low.
input: retrieved optical thicknesses for the ICI channels, model parameters (see entry *new channel selection* in Table 3.4 and (see entry *channel selection* in Table 3.3))
output: updated channel mask

3.5 Algorithm input

3.5.1 Primary sensor data

The primary input consists of calibrated and geolocated radiances for all ICI channels.

3.5.2 Static auxiliary data

The static auxiliary data required for the algorithm are surface altitude and type. The Level1B data are assumed to contain land fraction information for each pixel geolocation, and this data are used together with dynamic data for a surface type classification.

3.5.3 Dynamic auxiliary data

Forecast data from ECMWF model

- atmospheric: pressure, temperature, and humidity.
- surface: skin temperature, pressure, wind speed and direction, sea ice concentration, and snow depth.

3.5.4 Retrieval database

A retrieval database is a crucial element of the ICI retrieval algorithm. The retrieval database consists of a sufficiently large set of atmospheric scenes, along with associated (simulated) measurements. The physics and variability must be representative of the real world, as it will be used by the retrieval algorithm to perform the mapping from measurement to IWP and other retrieval products. The retrieval database can be divided into two parts. Both parts, basically, consists of the same set of atmospheric scenes and associated simulated measurements. The difference is that the first part describes each scene in detail, while the second part essentially only describes the retrieval parameters (e.g. IWP) and associated (simulated) measurements for each state of the first part of the retrieval database. The retrieval algorithm only need to use the second part of the retrieval database, which simply is a file as described in Appendix A. Further important aspects of the retrieval database and a method to develop such a database is also described in Appendix A.

3.5.5 Retrieval algorithm parameters

The ICI retrieval algorithm requires a number of setting parameters. The retrieval algorithm can be divided into two main modules, one preprocessing module (see Sect. 3.4.1) and one module (MCI-box) responsible for the actual retrieval calculation (see Sect. 3.4.2). These two modules are composed of sub-modules, and Table 3.3 and Table 3.4 list model input parameters for those sub-modules which require model input parameters.

Table 3.3: Retrieval algorithm parameters for preprocessing sub-modules.

Module	Parameter / description
extract EWMWF and surface data	• *D.extract_ecmwf_and_surface_data.minimum_snow_depth*: a scalar [m] minimum snow depth value (Eq. 3.14). Example: 0.05. • *D.extract_ecmwf_and_surface_data.minimum_fraction_value*: a scalar minimum fraction value (c_{min} in Eq. 3.15). Example: 0.95.
bias correction	• *D.bias_correction.offset*: a list describing offset [K] of the various ICI channels (Eq. 3.13). Example: [0, 0, 0, 0, 0, 0, 0, 0, 0, 0, 0], i.e no offset. The first and second item in the list represent ICI channel 1 and 2, and so on. • *D.bias_correction.scale*: a list describing scale errors [-] of the various ICI channels (Eq. 3.13). Example: [1, 1, 1, 1, 1, 1, 1, 1, 1, 1, 1], i.e no scale erros, and the first and second item in the list represent ICI channel 1 and 2, and so on.
modify humidity	• *D.modify_humidity.rh_value*: a scalar fixed relative humidity value [%] to use in RTTOV simulation. Example: 50.

Continued on next page

Table 3.3 – continued from previous page

Module	Parameter / description
channel selection	• *D.channel_selection.use_channels*: a mask list describing which ICI channels to possibly use in the retrieval calculation. Example: [1, 1, 1, 1, 1, 1, 1, 1, 1, 1, 1], i.e use all channels. The first and second item in the list represent ICI channel 1 and 2, and so on. • *D.channel_selection.tao_min_water*: a threshold optical thickness value for observations geolocated over a water surface (Eq. 3.17 and Eq. 3.30). Example: 1. • *D.channel_selection.tao_min_ice*: a threshold optical thickness value for observations geolocated over an ice surface (Eq. 3.17 and Eq. 3.30). Example: 3. • *D.channel_selection.tao_min_snow*: a threshold optical thickness value for observations geolocated over a snow surface (Eq. 3.17 and Eq. 3.30). Example: 3. • *D.channel_selection.tao_min_mixed*: a threshold optical thickness value for observations geolocated over a mixed surface type (Eq. 3.17 and Eq. 3.30). Example: 3. • *D.channel_selection.tao_min_land*: a threshold optical thickness value for observations geolocated over a land surface (Eq. 3.17 and Eq. 3.30). Example: 3.
obviously clearsky	• *D.obviously_clearsky.dt*: A list describing threshold values ([K]) for the various ICI channel for the clearsky test (Eq. 3.18). Example: 3·NEΔT or 3 * [0.8, 0.8, 0.8, 0.7, 1.2, 1.3 1.5, 1.4, 1.6, 2.0, 1.6], where the first and second item in the list represent NEΔT of ICI channel 1 and 2, and so on. • *D.obviously_clearsky.channel_group*: A list of lists describing group of ICI channels and priorities of the channels to be used in the obviously clearsky test (Eq. 3.19). Example: [[1, 2, 3], [4], [5, 6, 7], [8, 9, 10], [11]], i.e. five groups of channels are defined, where the first group of channels contains ICI channel 1, 2, and 3. Channel 1 has the highest priority in group 1.

Table 3.4: Retrieval algorithm parameters for mci-box sub-modules.

Module	Parameter / description
basic mci_box setting	• *D.mci_box.database_file*: the path to a retrieval database file (see Appendix A.5 for anticipated database file format and content). • *D.mci_box.do_clearsky_retrieval*: a flag describing if measurements that are classified as "obvioulsy clear sky" shall be inverted or not. Example: 0, i.e do no retrieval calculation for those measurements. • *D.mci_box.do_update_channel_mask*: a flag describing if the new channel selection module of the MCI-box shall be applied and thereby possibly a second retrieval calculation will be performed. Example: 1, i.e. apply new channel selection module.
calculate dy	• *D.calculate_dy.nedt*: a list describing NEΔT [K] of the ICI channels (Eq. 3.11). Example: [0.8, 0.8, 0.8, 0.7, 1.2, 1.3 1.5, 1.4, 1.6, 2.0, 1.6]. The first and second item in the list represent ICI channel 1 and 2, and so on. • *D.calculate_dy.sigma_noise_simulation*: list of scale errors of simulated cloud signals, for the various ICI channels, of states in the retrieval database file (parameter c in Eq. 3.11). Example: 0.03 * [1, 1, 1, 1, 1, 1, 1, 1, 1, 1, 1]. The first and second item in the list represent ICI channel 1 and 2, and so on. • *D.calculate_dy.emissivity_error*: a list of surface emissivity errors of clear sky simulation. ($\Delta\varepsilon_j$ in Eq. 3.11) for various surface types. Example: [0.005, 0.03, 0.03, 0.05, 0.03]. The first to forth value represent water, ice, snow, mixed, and land surfaces in described order.

Continued on next page

Table 3.4 – continued from previous page

Module	Parameter / description
extract from database	• *D.extract_from_database.minimum_number_of_states*: minimum number of states that can be extracted from database (Eq. 3.21). Example: 500. • *D.extract_from_database.maximum_number_of_states*: maximum number of states that can be extracted from database. Example: 50000. • *D.extract_from_database.do_preselection_dtb*: a flag describing if a filter shall be applied (brightness temperature difference) when selecting states from database or if all states shall be selected (Eq. 3.21). Example: 1, i.e apply the filter • *D.extract_from_database.channel_group*: A list of lists describing group of ICI channels and priorities of the channels to be used in the selection (see Eq. 3.22). Example: [[1, 2, 3, 11], [4], [5, 6, 7, 8, 9, 10]], i.e. 3 groups of channels are defined, where the first group of channels contains ICI channel 1, 2, 3, 11. Channel 1 has the highest priority in group 1. • *D.extract_from_database.search_radius*: scalar search radius value (parameter s in Eq. 3.21). Example: 4. • *D.extract_from_database.do_preselection_surfprop*: a flag describing if a filter depending on surface properties shall be applied when selecting states from database (Eq. 3.21). Example: 1, i.e apply surface property filter. • *D.extract_from_database.surfprop_parameters*: a list describing which surface properties to take into account of by the selection filter (Eq. 3.21). Example: ['surface_type', 'surface_pressure', 'surface_wind_speed', 'surface_temperature'].

Continued on next page

Table 3.4 – continued from previous page

Module	Parameter / description
extract from database	• *D.extract_from_database.surface_pressure_max_diff*: a scalar [Pa] describing acceptable surface pressure difference between observation and database state to be selected (Eq. 3.21). Example: 1000. • *D.extract_from_database.surface_temperature_max_diff*: a scalar [K] describing acceptable surface temperature difference between observation and database state to be selected. Example: 2 • *D.extract_from_database.surface_wind_speed_max_diff*: a list (five elements corresponding to water, ice, snow, mixed, and land surface type) [m/s] describing acceptable surface wind speed difference between observation and database state to be selected (Eq. 3.21). Example: [5, 50, 50, 50, 50]. • *D.extract_from_database.acceptable_surface_types*: a list of lists describing acceptable surface types for each surface type (see Eq. 3.21). Example: [[0], [1, 2], [1, 2], [1, 2, 3, 4], [4]]. The first to last list is valid for water, ice, snow, mixed, and, land surface and water = 0, ice = 1, snow = 2, mixed = 3, and land = 4.
recovery iteration	• *D.recovery_iteration.min_channels*: scalar minimum number of channels to use in retrieval. Example: 1. • *D.recovery_iteration.max_iter*: scalar maximum number of times to increase search radius. Example: 1.
increase search radius	• *D.increase_search_radius.scale*: list of scale factors describing how much the observation system noise will be increased in each iteration for each ICI channel (see Eq. 3.26). Example: [$\sqrt{2}$, $\sqrt{2}$, $\sqrt{2}$, $\sqrt{2}$, $\sqrt{2}$, $\sqrt{2}$, $\sqrt{2}$, $\sqrt{2}$, $\sqrt{2}$, $\sqrt{2}$, $\sqrt{2}$]. The first and second item in the list represent ICI channel 1 and 2, and so on.

Continued on next page

Table 3.4 – continued from previous page

Module	Parameter / description
remove channels	• *D.remove_channels.channel_priority*: priority list of how the channels shall be removed (Eq.3.27). Example: [10, 9, 8, 11, 7, 3, 6, 2, 5, 1, 4], i.e. ICI channel 10 and 4 will be removed first and last, respectively.
check weights	• *D.check_weights.n_min*: minimum number of database hits accepted by the retrieval (Eq. 3.25) . Example: 50. • *D.check_weights.search_radius*: scalar search radius value (parameter s in Eq. 3.24). Example: 2. • *D.check_weights.n_max*: maximum number of states used for retrieval. Example: 50000.
compute output	• *D.compute_output.parameters*: a list describing which parameters to be retrieved from the observation. Example: ['iwp', 'dmean', 'zcloud', 'icehabit', 'optical_depth', 'cwv', 'lwp']. • *D.compute_output.iwp_cdf*: a list describing IWP CDF levels to be retrieved. Example: [0.05, 0.16, 0.5, 0.84, 0.95]. • *D.compute_output.dmean_cdf*: a list describing D_{mean} CDF levels to be retrieved. Example: [0.05, 0.16, 0.5, 0.84, 0.95]. • *D.compute_output.zcloud_cdf*: a list describing Z_{cloud} CDF levels to be retrieved. Example: [0.05, 0.16, 0.5, 0.84, 0.95]. • *D.compute_output.cwv_cdf*: a list describing *cwv* (column water vapour) CDF levels to be retrieved. Example: [0.05, 0.16, 0.5, 0.84, 0.95]. • *D.compute_output.lwp_cdf*: a list describing *lwp* (liquid water path) CDF levels to be retrieved. Example: [0.05, 0.16, 0.5, 0.84, 0.95]. • *D.compute_output.optical_depth_cdf*: a list describing cloud optical depths CDF levels to be be retrieved. Example: [0.5].

Continued on next page

Table 3.4 – continued from previous page

Module	Parameter / description
new channel selection	• *D.new_channel_selection.cloud_optical_depth_factor*: a scalar factor used to give clear sky and cloud optical depth comparable importance (parameter c in Eq. 3.30). Example: 10.

3.6 Algorithm output

3.6.1 Main retrieval and auxiliary parameters

The ICI retrieval algorithm generates the following output quantities

- IWP and IWP error estimate. The posterior CDF evaluated at specified levels: (see Sect. 3.1.4 for more details).
- D_{mean} and a D_{mean} error estimate. The posterior CDF, on the additional condition that IWP > 0, evaluated at specified levels (see Sect. 3.1.4 for more details).
- Z_{mean} and a Z_{mean} error estimate. The posterior CDF, on the additional condition that IWP $> 0[kg/m^2]$ evaluated at specified levels (see Sect. 3.1.4 for more details).
- Auxiliary parameters
  - retrieval algorithm quality flags: status (succes, failure, or obviously-clearsky), number of database hits, number of channels used in retrieval, parameters describing the final iteration state of retrieval, i.e number of iterations for "*increasing search radius*", "*remove channel*", and "*any reason to redo with more channels*"?
  - Tb_{cs} and τ_{cs} (from rttov calculations)
  - Optional: Retrieved cloud optical depths ($\tau_{cloud,med}$) and cloud particle model probability
  - Optional: Retrieved liquid water path and total column water vapor. These parameters can be retrieved in analogously to how IWP is retrieved.
  - Latitude and longitude for the satellite footprint
  - Latitude and longitude corresponding to Z_{mean}, i.e the position where the line of sight between ICI and the satellite footprint is located Z_{mean} m above mean sea level.
  - Time for the measurement.

3.6.2 Quality of retrieval calculation

Generally, the retrieval calculation is strongly dependent on the quality of the retrieval database. The quality of the retrieved parameters will clearly be poor if the variability of the atmospheric states and corresponding simulated measurements does not reflect the true nature. There will also be a retrieval error related to the finite size of the retrieval database. Ideally, the retrieval database should contain thousands of states that match each possible ICI measurement. The quality of the uncertainy estimate of retrieval calculation will clearly be poor if there is no or only a few database states that match a given measurement. This is true if the reason behind this is either due to the fact that the database does not reflect reality or that the database has a limited size.

A quality measure of the ICI IWP product is calculated for each individual retrieval. This quality measure is effectively determined from the match between the observation and database

Table 3.5: Quality of retrieval calculation.

Quality level	Description
0 (highest quality)	all channels used, no increased search radius applied
1	all channels used, increased search radius applied
2	one to three channels removed
3	four to six channels removed
4	seven to nine channels removed
5	one channel used, no increased search radius applied
6 (lowest quality)	one channel used, increased search radius applied

states, or more specifically from the number of channels that was used in the retrieval calculation and the final state of the "recovery iteration", as described in Table. 3.5. That is, the highest quality is given to mesurements where there is a significant amount of database states that match the observation, and the lowest quality is given to observations where only one channel could be used in order to find a reasonable amount of database matches.

Figure. 3.8 displays statistic of quality estimates determined from a retrieval simulation. It is stressed that the simulation is based on a retrieval database, developed for a testing of algorithm purpose, having a smaller size than what is anticipated to be the case for an "operational" database.

Anyhow, it can be seen that the majority of retrievals have a high quality (0 or 1) for states with an IWP $\leq 1[kg/m^2]$. The retrieval quality is low for a significant amount of states having an IWP $\geq 10[kg/m^2]$. The explanation to this is basically related to the fact that the retrieval database contains less states having high IWP than low IWP, as the distribution of states follows the *a priori* distribution. It is possible to deploy a retrieval database having a more optimised distribution of states w.r.t the ICI retrieval and to still conform to a Bayesian principle as discussed in Sect. 3.1.2.

Even though, the retrieval quality for states with a very high IWP may be low, the observed cloud signal is in general very high for these observations. Thus, it is in general no doubt that the IWP is high for those states, but the realibility of the uncertainty estimate is low. This limitation is clearly severe for applications where the exact uncertainty estimate is important, but for application where it is not crucial to distinguish if e.g. the IWP is above 10 or $20[kg/m^2]$, the degraded quality is of less importance.

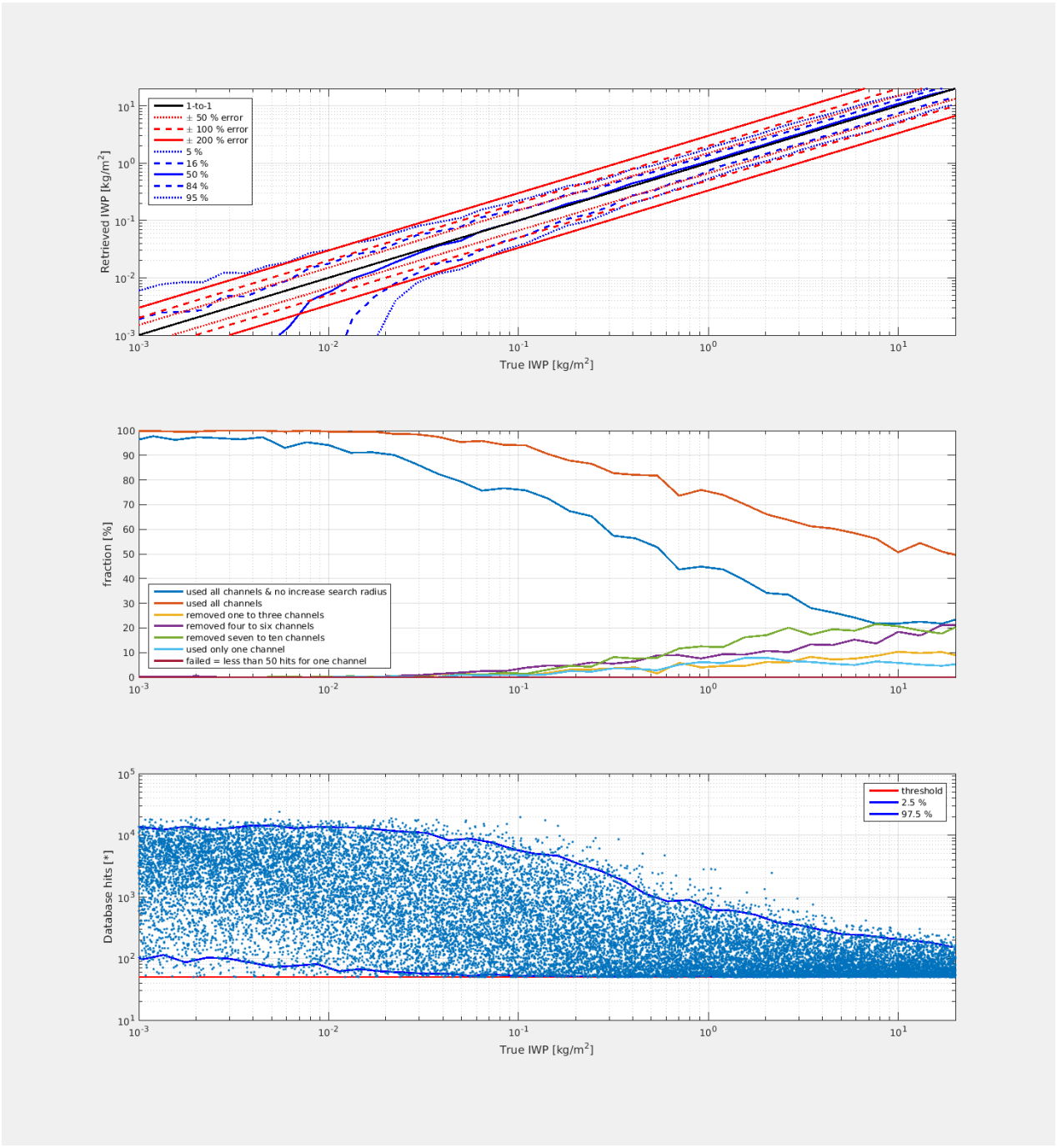

Figure 3.8: Some retrieval quality estimates for simulated observations associated with a warm surface temperature ([290 - 310 K]) and a test retrieval database of limited size (see text for more details).

Chapter 4

Future development

4.1 Work to be done

4.1.1 Retrieval algorithm

This document describes the details of the components, including the dataflow between components, of the ICI retrieval algorithm. These details and the dataflow are considered to be stable, and it is anticipated that no major future refinement is required, although it should be mentioned that the retrieval algorithm has never been applied operationally on any observations before. The retrieval algorithm contains a number of model parameters (Sect. 3.5). The exact setting of the values of these model parameters requires further work. Thus, more testing of the algorithm, including to apply it on observations from instruments in service today, and to perform more retrieval simulations, is required in order to set the retrieval algorithm parameters properly.

4.1.2 Retrieval database

The method to generate a retrieval database for ICI was "validated" by comparing statistics of simulated and real ATMS measurements (Appendix A.4). The agreement was considered to be high, but deviations could also clearly be seen in data, and possible explanations were given. Future developments of the ICI retrieval database should include:

- Create a larger retrieval database. Create a database based on several years of CloudSAT data for all geographical regions.
- Characterization of beamfilling effects for ICI observation. Ideally the retrieval database should contain states with a 3-D variation, in order to completely resolve beamfilling issues. Beamfilling effects are likely to be most important for deep convective clouds and relatively small for most other clouds. Thus, the retrieval database should probably at least include 3-D varying states for deep convective clouds.
- Inclusion of mixed-phase clouds/particles.

- Inclusion of more ice particle habits, including oriented ice particles. This includes to simulate the polarization effects of horizontally aligned particles on ICI measurements. This is not only of concern for the 243.2 ± 2.5 GHz and 664.0 ± 4.2 GHz channels that measure both H and V polarization, but also for all other channels that only measure V polarization. A retrieval bias will be introduced, if not the effect of non randomly oriented particles on ICI observation is taken into account.
- A better surface emissivity modeling, when such model/data becomes available for ICI channels.
- Variation of the cloud ice PSD. It is important that the cloud ice PSD of the database states are varied according to reality, in order to generate an accurate error estimate of the retrieval.

Acknowledgment

The definition of this retrieval algorithm would not have been possible without various input. Most importantly, the simulations to create the retrieval database require recent development of the ARTS software and its associated scattering database, and the community around these tools is thanked for its contributions. A large fraction of the work was performed inside projects founded by the Swedish National Space Board. The scattering database development is also supported by EUMETSAT.

Bibliography

S. J. Abel and I. A Boutle. An improved representation of the raindrop size distribution for single-moment microphysics schemes. *J. Quant. Spectrosc. Radiat. Transfer*, 128:2152–2162, 2012. doi: 10.1002/qj.1949.

C. Davis, C. Emde, and R. Harwood. A 3D polarized reversed monte carlo radiative transfer model for mm and sub-mm passive remote sensing in cloudy atmospheres. *IEEE T. Geosci. Remote*, 43(6):1096–1101, May 2005.

C. Davis, K. F. Evans, S. A. Buehler, and D. L. Wu. 3-d polarised simulations of space-borne passive mm/sub-mm midlatitude cirrus observations: a case study. *Atmos. Chem. Phys.*, 43 (6):4149–4158, 2007.

A. M. Dzambo and D. D. Turner. Characterizing relative humidity with respect to ice in midlatitude cirrus clouds as a function of atmospheric state. *J. Geophys. Res.*, 121:12253–12269, 2016. doi: 10.1002/2015JD024643.

C. Emde, S. A. Buehler, C. Davis, P. Eriksson, T. R. Sreerekha, and C. Teichmann. A polarized discrete ordinate scattering model for simulations of limb and nadir longwave measurements in 1D/3D spherical atmospheres. *J. Geophys. Res.*, 109(D24):D24207, 2004. doi: 10.1029/2004JD005140.

P. Eriksson, S. A. Buehler, C. P. Davis, C. Emde, and O. Lemke. ARTS, the atmospheric radiative transfer simulator, version 2. *J. Quant. Spectrosc. Radiat. Transfer*, 112:1551–1558, 2011. doi: 10.1016/j.jqsrt.2011.03.001.

P. Eriksson, R. Ekelund, J. Mendrok, M. Brath, O. Lemke, and S. A. Buehler. A general database of hydrometeor single scattering properties at microwave and sub-millimetre wavelengths. *Earth Syst. Sci. Data Discuss.*, 2018. doi: 10.5194/essd-2018-23.

K. F. Evans and G. L. Stephens. Microwave radiative transfer through clouds composed of realistically shaped ice crystals. Part ii: remote sensing of ice clouds. *J. Atmos. Sci.*, 52: 2058–2072, 1995.

K. F. Evans, S. J Walter, A. J Heymsfield, and G. M. McFarquhar. Submillimeter-wave cloud ice radiometer: Simulations of retrieval algorithm performance. *J. Geophys. Res.*, 107:D2.1–D2.22, 2002.

K. F. Evans, J. R. Wang, D. O'C Starr, G. Heymsfield, L. Li, L. Tian, R. P. Lawson, A. J. Heymsfield, and A. Bansemer. Ice hydrometeor profile retrieval algorithm for high-frequency microwave radiometers: application to the CoSSIR instrument during TC4. *Atmos. Meas. Tech.*, 5:2277–2306, 2012. doi: 10.5194/amt-5-2277-2012.

P. R. Field, A. J. Heymsfield, and A. Bansemer. Snow size distribution parameterization for midlatitude and tropical ice clouds. *J. Atmos. Sci.*, 64:4346–4365, 2007. doi: 10.1175/2007JAS2344.1.

A. J. Geer and F. Baordo. Improved scattering radiative transfer for frozen hydrometeors at microwave frequencies. *Atmos. Meas. Tech.*, 7:1839–1860, 2014. doi: 10.5194/amt-7-1839-2014.

C Jiménez, S.A Buehler, B. Rydberg, P. Eriksson, and K. F. Evans. Performance simulations for a submillimetre-wave satellite instrument to measure cloud ice. *Q. J. R. Meteorol. Soc.*, 133(S2):129–149, 2007. doi: 10.1002/qj.134. URL `http://dx.doi.org/10.1002/qj.134`.

G. M. McFarquhar and A. J Heymsfield. Parameterization of tropical cirrus ice crystal size distributions and implications for radiative transfer: results from CEPEX. *J. Atmos. Sci.*, 54:2187–2200, 1997. doi: 10.1175/1520-0469(1997)054⟨2187:POTCIC⟩2.0.CO;2.

B. Rydberg, P. Eriksson, S. A. Buehler, and D. P. Murtagh. Non-gaussian bayesian retrieval of tropical upper tropospheric cloud ice and water vapour from Odin-SMR measurements. *Atmos. Meas. Tech.*, 2(2):621–637, 2009. ISSN 1867-1381. URL `www.atmos-meas-tech.net/2/621/2009/`.

D. Sonntag. Advancements in the field of hygrometry. *Met. Zeit.*, 3:51–56, 1994.

Appendices

Appendix A

ICI training database

A.1 Important aspects

The training database is a crucial element of the ICI retrieval algorithm. The training database consists of a sufficiently large set of atmospheric scenes, along with associated (simulated) measurements. The physics and variability must be representative of the real world, as it will be used by the retrieval algorithm to perform the mapping from measurement to IWP and other retrieval products. The training database can be divided into two parts. Both parts, basically, consists of the same set of atmospheric scenes and associated simulated measurements. The difference is that the first part describes each scene in detail, while the second part essentially only describes the retrieval parameters (e.g. IWP) and associated (simulated) measurements for each state of the first part of the retrieval database. The retrieval algorithm only need to use the second part of the retrieval database, which simply is a file (Appendix A.5).

Main considerations for the generation of the training database are described below:

- **The retrieval database must be sufficiently large.** This means that for each possible measurement of ICI, there should be a number of states in the retrieval database that match the measurement.
- **The states in the retrieval database should ideally be sampled from the *a priori* probability distribution.** This is not trivial to follow strictly, as the *a priori* probability distribution of all variables are not perfectly known.
  - **Cloud ice structures** (of mass contents and underlying microphysical properties) **must have a realistic variation.** Ideally the training database should consist of 3-D varying atmospheric states, as it is clear that 3-D radiative transfer effects (or beam filling effects) can have an impact on ICI measurements [Davis et al., 2007]. However, 3-D radiative transfer scattering simulations is a computational expensive task, and since the training database must be sufficiently large, it is presently not an option to deal with 3-D clouds.
  - **A range of ice particle habits must be included in the training database.** Particles in ice clouds can have very complex shapes in nature, and it should be clear that it is impossible to include all potential shapes in the ICI training database. In

fact, it is in practice only possible to include a few particle habits, as the needed single scattering properties (SSP) are only available for a few particle habits. The SSP of complex shaped particles can be obtained from discrete dipole approximation calculations. However, it is extremely computational demanding to obtain the SSP necessary for ICI-simulations. Anyhow, the most important thing is not to include all potential shapes, but to include a few types that covers the range of the "scattering strength" of natural occurring ice particle habits, for each cloud and precipitation type.

- **Liquid clouds and rain must be included**, since liquid clouds and rain occasionally have an impact on ICI measurements. Liquid water path and rain are not attempted to be retrieved by the ICI retrieval algorithm, but the retrieval algorithm must be able to handle the impact of liquid clouds and rain on ICI measurements. However, a totally correct description of liquid clouds and rain, in the training database, is less critical than for ice clouds.
- **Weather information** (pressure, temperature, humidity) must have a realistic variation.
- Some of the ICI channels are occasionally sensitive to the **surface emissivity**, and the surface emissivity must be modeled in a realistic way, if the retrieval should be able to correctly handle such measurements. However, a complete surface emissivity model for land and ocean is not available for the ICI channels. The retrieval algorithm will therefore use channels that are significantly influenced by the surface with care, and the surface emissivity modeling is accordingly less critical.

Algorithms to create training databases for the IWP retrieval from sub-mm radiometric measurements have earlier been presented in e.g. Rydberg et al. [2009] and Evans et al. [2012]. Cloud profiling radar (CPR) data from CloudSAT constitute the main *a priori* source for cloud structure within both of these algorithms. Rydberg et al. [2009] present an algorithm that creates synthetic atmospheric states with three-dimensional varying cloud structures, based on CloudSAT data, but with an oversimplified cloud microphysics variability. Evans et al. [2012] present an algorithm that creates atmospheric states having only 1-D (vertical) varying cloud structures, primarily based on CloudSAT data, but with a high microphysical variability, but only for tropical conditions. Thus, both methods have limitations, and there is a need to develop a new method optimized for ICI. The approach used to generate the database used to test the retrieval algorithm is described below.

A.2 Input data

CloudSAT Cloud Profiling Radar data

The Cloud Profiling Radar (CPR) onboard CloudSAT is a 94-GHz nadir-looking radar that measures the power backscattered by clouds as a function of distance from the radar. CloudSAT follows a 705-kilometer circular sun-synchronous polar orbit with an ascending node around 13:30. The resolution of CPR data is approximately 500 m vertically, 1.3 km across-track, and

Table A.1: Cloud partcile models.

id	hydrometeor	size distribution	habit	region
11	snow	f07t, [Field et al., 2007]	evans-snow-aggregate	tropics
13	snow	f07t, [Field et al., 2007]	liu-sector-snowflake	tropics
14	snow	mh97, [McFarquhar and Heymsfield, 1997]	plate-aggregate-mix	tropics
21	snow	f07m, [Field et al., 2007]	evans-snow-aggregate	mid and high latitudes
24	snow	mgd [Geer and Baordo, 2014]	evans-snow-aggregate	mid and high latitudes
25	snow	mgd [Geer and Baordo, 2014]	hong-8-column-aggregate	mid and high latitudes
-	rain	abel12, [Abel and Boutle, 2012]	sphere	global

1.7 km km along-track. The minimum detectable equivalent radar reflectivity is approximately -27 dBZ and the dynamic range is 70 dBZ. This study uses radar reflectivities from the 2B-GEOPROF product and cloud class classification from the 2B-CLDCLASS product provided by the CloudSat Data Processing Center, as this data are considered to be the best available cloud structure information with near global coverage.

Surface and atmospheric data

ERA-Interim is a global atmospheric reanalysis. Its coverage starts from 1979, and is continuously updated in real time, and serves as source of weather data (pressure, temperature, humidity, and liquid water content) and surface skin temperature and wind speeed and direction, for the generation of the scenes in the training database. A land sea mask based on the "Global Self-consistent Hierarchical High-resolution Geography Database" (GSHHG) is used to categorize surface type (land or water), and surface topography data, provided by the CloudSAT 2B-GEOPROF product, are used as surface altitude information.

Cloud particle models

Seven different cloud particle models was used in this study (defined in Table A.1). A particle model is here defined as a combination of a cloud particle size distribution parameterisation and habit (or shape, see Fig. A.1 for some examples). Six of the particle models are used to represent cloud ice / snow particles, three of these are used for tropical conditions while the other three for mid and high latitudes. One single model is used to represent rain globally. The regional validity is primarily related to the location of the associated measurement campaign from where the various size distribution parameterisations were derived, although also the various habits were attempted to be selected based on best guesses for the various regions. The single scattering properties (SSP) of the various habits used are calculated for randomly oriented particles for all of the habits (see Eriksson et al. [2018] for more details).

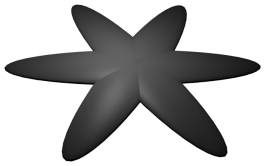

(a) Sector snow flake.

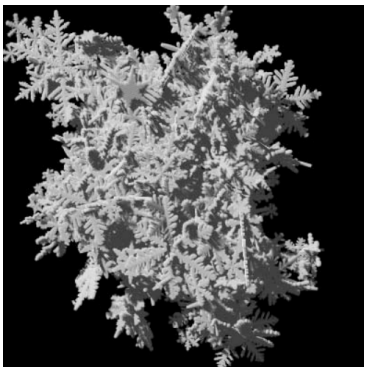

(b) Evans snow aggregate.

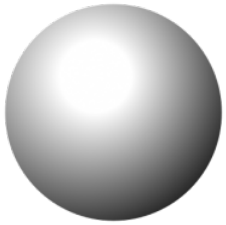

(c) Rain.

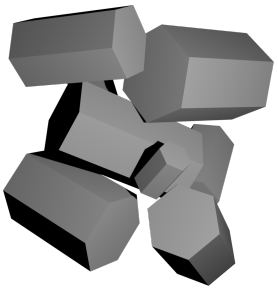

(d) Hong aggregates.

Figure A.1: Example images of the cloud particle habits, sector snowflake, Evans snow aggregate, rain, and Hong aggregates used in the ICI training database.

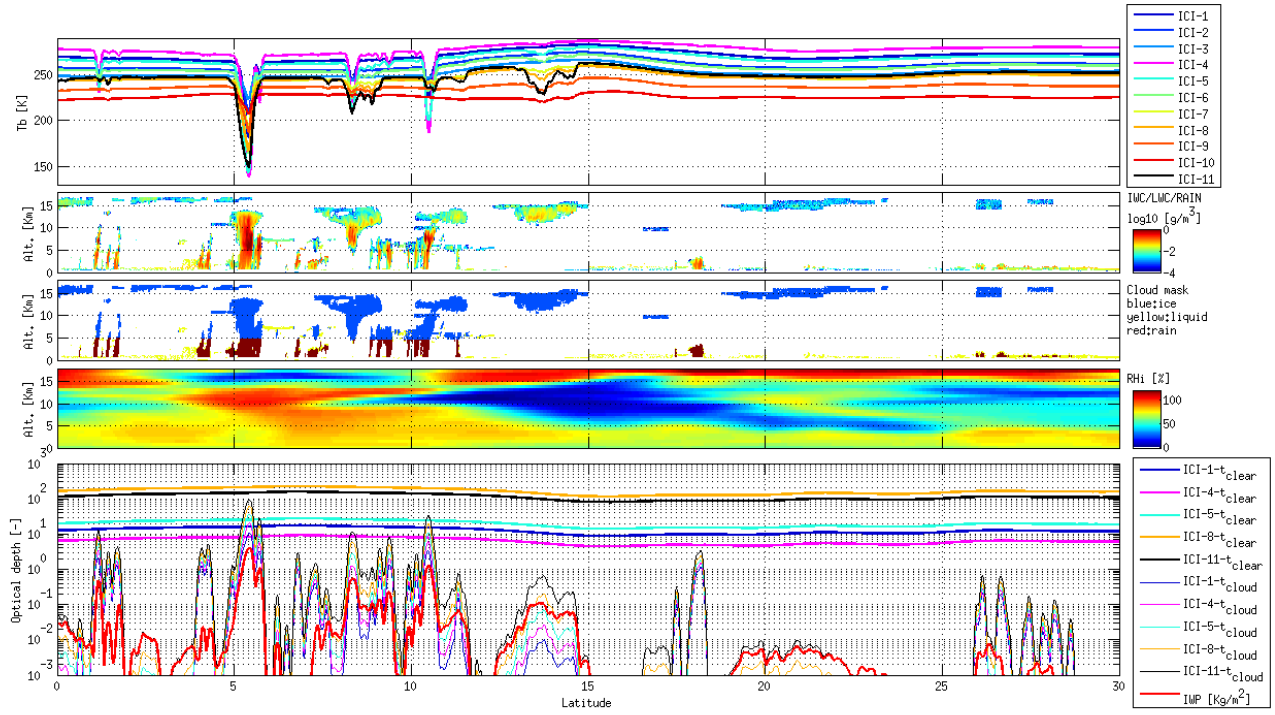

Figure A.2: An example of an atmospheric scene (for tropical conditions) and simulated data. The upper panel shows simulated measurements of ICI. The second and third panel show cloud water content (in various phases), and cloud phase mask, respectively. The bottom panel show clear sky and cloud optical thicknesses for ICI channels 1, 4, 5, 8 and 11, and IWP.

A.3 Generation of the training database

In this section we present a method that effectively creates a training database consisting of 2-D varying atmospheric/cloud states and associated simulated measurements. Two examples of scenes are displayed in Figure A.2 (for tropical condition) and Figure A.3 (for mid-latitude condition). The basic idea of the database generation scheme is that 2-D varying atmospheric scenes, including cloud features, are constructed from radar reflectivity, ERAInterim data, and particle model data. ICI measurement simulations are then performed by assuming that ICI measure within the CloudSAT orbital plane. The radiative transfer model ARTS is applied to simulate ICI measurements in a slant down-looking geometry. The simulations are performed in a pseudo 2-D mode.

Atmospheric scenes

Cloud features and categorization

Three types of cloud categories are possibly included in a scene, and these are:

- ice cloud: consisting of non-spherical ice/snow particles,
- rain: consisting of large spherical water particles,

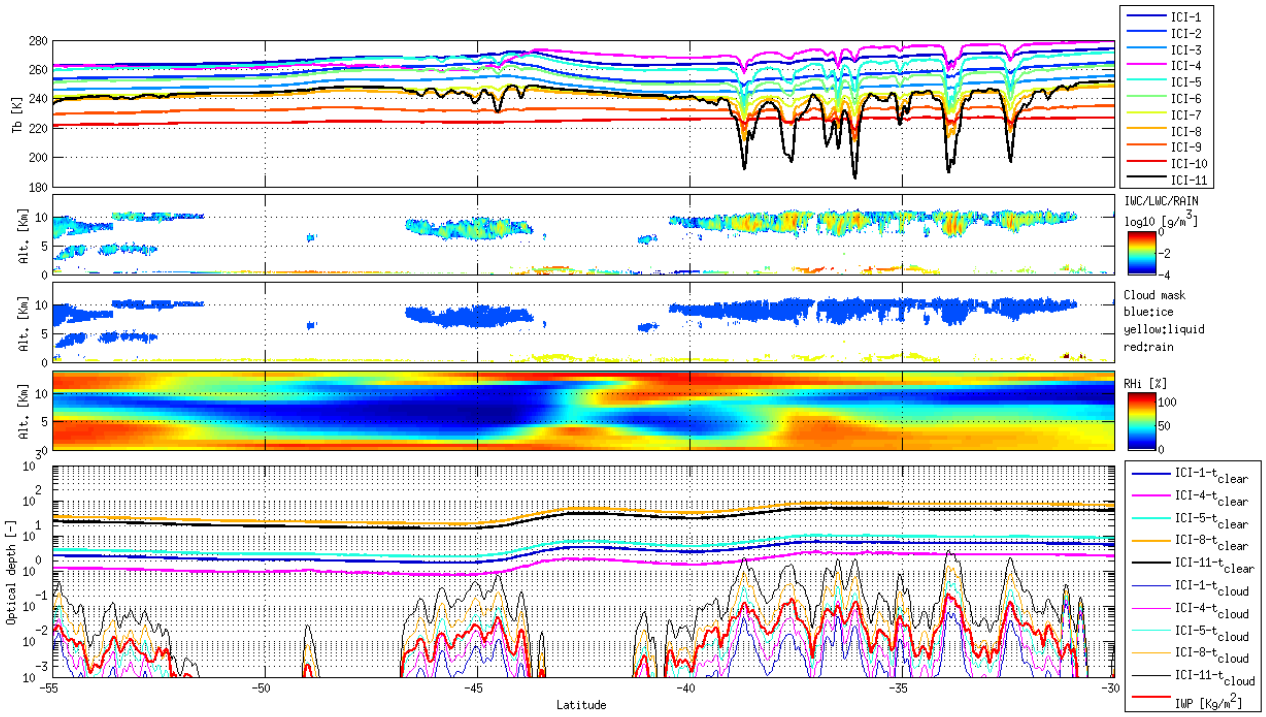

Figure A.3: As Figure A.2 but for mid-latitude conditions.

- liquid cloud: consisting of small spherical water particles,

Radar reflectivity from the CPR onboard CloudSAT serves as the main data source for building up 2-D varying atmospheric scenes (see Figure A.2). Radar reflectivity from a part of a given CloudSAT orbit is used by the scene generation scheme. ERAInterim data are then sampled at the geolocation of the radar data. Snow (or ice) and rain water content fields are then recreated from this data, by assuming that one of the snow and the only rain particle model (see Sect. A.2) are valid for this particular scene, by using precalculated lookup tables that relates cloud water content as function of radar reflectivity and temperature (the inversion also takes into account of attenuation). No snow particle model have a higher priority than any other, and the various snow particles models are included in an equal amount of states. The snow / rain water inversion scheme applies a sharp "melting level", determined by temperature, for a given scene. That is, the retrieved cloud water content is of hydrometeor type snow and rain if the temperature is below and above, respectively, a "melting level" temperature. The "melting level" temperature is fixed for a given scene, but is allowed to vary (263.15 ± 12 K) between scenes.

The reason for including several snow particle models in the database is to cover a wide variability of cloud microphysics. Retrieval uncertainties derived by the ICI retrieval algorithm will otherwise tend to be too small. It should anyhow be noted that it is far from a trivial task to deal with microphysical variability in a realistic way. In true life a cloud structure may contain a mixture of cloud particle models (as defined here), while the important point of the ICI database is to represent cloud structure average particle model in a realistic way. Hence, it is possible that the current scheme overemphasize the variablity as it assigns a single

snow particle model to a given cloud structure, which then effectively will lead to that retrieval uncertainties are overestimated.

The sensitivity of the CPR to liquid clouds are weak, therefore liquid water content (LWC) fields are primarily taken from ERAInterim. However, the ERAInterim liquid water content field is slightly adjusted and set to zero if temperature is below 235 K, or altitude is above 10 km, or radar reflectivity is below -28 dBZe. The size of the particles in liquid clouds are typically around 10 μm (while between 0.5–4 mm for rain), and the interaction with radiation is dominated by absorption effects at frequencies around ICI channels. The absorption is proportional to the mass of the particles and independent of the size distribution. Liquid clouds are therefore included as an absorbing species in the radiative transfer simulations, and no size distribution or habit is assigned to the particles.

Weather and background data

Atmospheric data (pressure, temperature, humidity) from ERA-Interim are used for the generation of the scenes in the training database, and data is interpolated to the geolocation of the radar data. The humidity field is slightly modified to take into account of the relatively low ERA-Interim resolution as compared to the CPR data. The modification is based on results on humidity variation in cirrus clouds as presented by Dzambo and Turner [2016] and data from the 2B-CLDCLASS product (cloud classification product). The relative humidity is set to vary from approximately 95 % RHi to 70 % RHi from cloud top to bottom for cloud features that are classified as cirus clouds. For nimbostratus and deep convective clouds the humidity is set to around 100 % RHi. The modification is done in a humidity conservation approach, i.e lowering the humidity (if necessary) outside the cloud features.

Surface data (skin temperature and wind speed) from ERA-Interim, a land ocean mask (GSHHG), and topography data are used for the generation of the scenes. Surface wind is effectively only important over water surfaces through its impact on surface emissivity, as described in Sect. A.3.

Forward model simulations

The radiative transfer simulations for the ICI traning database are performed by version 2.3 of the Atmospheric Radiative Transfer Simulator (ARTS) [Eriksson et al., 2011]. ARTS includes a number of scattering solver modules, e.g; (1) a Discrete Ordinate ITerative (DOIT) algorithm [Emde et al., 2004], (2) a reverse Monte Carlo (MC) algorithm [Davis et al., 2005], (3) a Discrete Ordinates Radiative Transfer Solver for a Multi-Layered Plane-Parallel Medium (DISORT), and (4) an adding and doubling plane-parallel fully-polarized module (rt4) [Evans and Stephens, 1995]. The MC module is in general the most accurate one, but it is also the most expensive module in terms of computational time.

The rt4 scattering module is used, for ICI measurement simulations (if the input atmosphere is cloudy, otherwise ordinary clear sky simulations are performed). The rt4 (and DISORT) module is considerable (order of magnitudes) faster than the other two modules. For unpolarised ICI simulations, the agreement between rt4 and the benchmark MC module is very high (well below 1 K for most cases).

The simulations are performed in a pseudo 2-D mode assuming that ICI measure within the CloudSAT/Calipso orbital plane (see Figure A.2). The independent pixel approximation technique is applied. That is, a number of pencil beam simulations for a 1-D varying atmosphere is performed, where the 1-D atmosphere is sampled along this line of sight from the 2-D atmosphere, for each footprint of ICI. The individual 1-D simulations are then weighted according to the ICI antenna response function. The simulations are performed for the center frequency of the two passbands of the ICI channels.

ARTS interface to FASTEM (parameterised ocean surface emissivity model) was applied for simulations over oceans and a specular reflective surface was used over land (with a randomized reflectivity, lognormal distributed around 0.1 with a standard deviation of 0.03).

For each simulation additional information is calculated and stored. A clear sky simulation is performed for each simulation, even if the atmosphere is cloudy, by masking out all hydrometeors in the simulation. Additionally, the relative humidity is set to a fixed value (50 %RHi) for these clear sky simulations. The clear and cloudy sky optical depths are also calculated for each simulation.

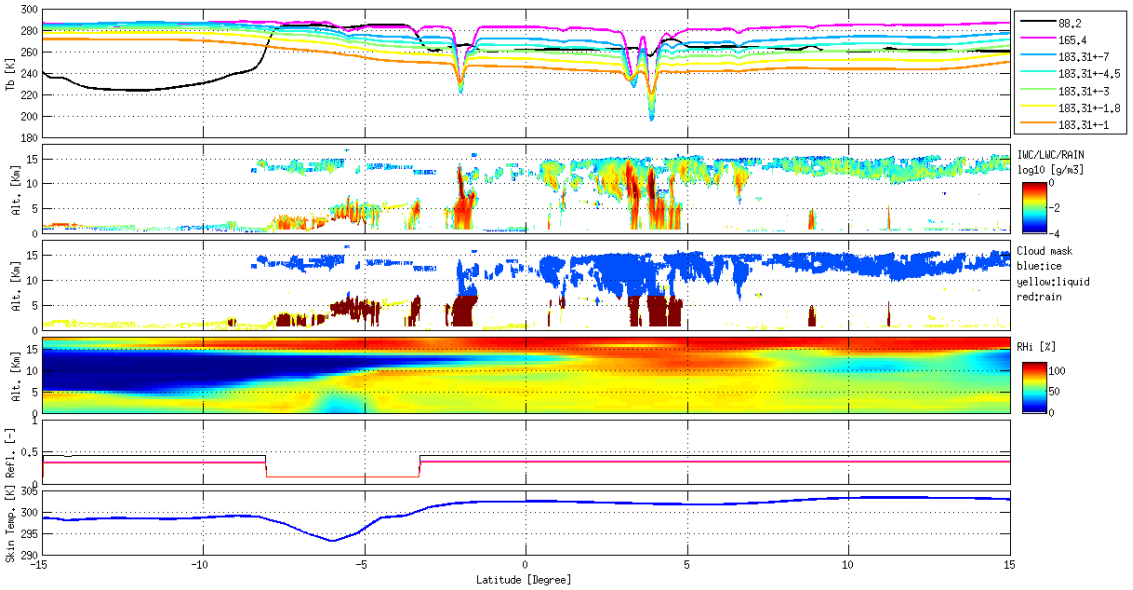

Figure A.4: An example of an atmospheric scene and measurement simulation. The upper panel shows simulated measurements of Advanced Technology Micirowave Sounder (ATMS), and the lower panels the underlying atmospheric and surface state. The second and third panel show cloud water content (in various phases), and cloud phase mask, respectively, mainly based on data from the DARDAR Level2 product. The two bottom panels show surface reflectivity and surface temperature. Simulations have been performed for the slant view of ICI and the atmospheric structure is plotted in a "tilted" way. That means that a measurement simulation, at a given latitude, is associated with a state at the same latitude.

A.4 Validation of the training database

A true validation of the training database is impossible to perform at this stage, but a basic test one can peform is to compare the simulated measurements of the training database to existing measurements. The Advanced Technology Microwave Sounder (ATMS) is a 22 channel scanning microwave sounder with channels operating at frequencies in the range from 23 – 183 GHz, and is here used for "validating" the simulations.

Figure A.5 displays a statistical comparison between simulations and ATMS measurements. To be clear, the simulations and measurements are not co-located but the probability density functions (PDFs) displayed in Figure A.5 should anyhow agree, as we are comparing the statistics of the two datasets from one month.

The agreement between simulations and measurements is excellent for ATMS channels 17 – 21 and brightness temperatures (TBs) above 200 K. Below 200 K there is a discrepancy between simulations and measurements (simulations are more frequent colder than observations). These cases correspond to measurements / simulations at or close to deep convective cores. The overestimation of ΔTb in the simulation can be due to beamfilling effects, not completely captured by the simulation. It might be that the deep convective cores tend to only partly "fill" the ATMS beam, whereas the core is smeared out over the complete beam in the simulation. The

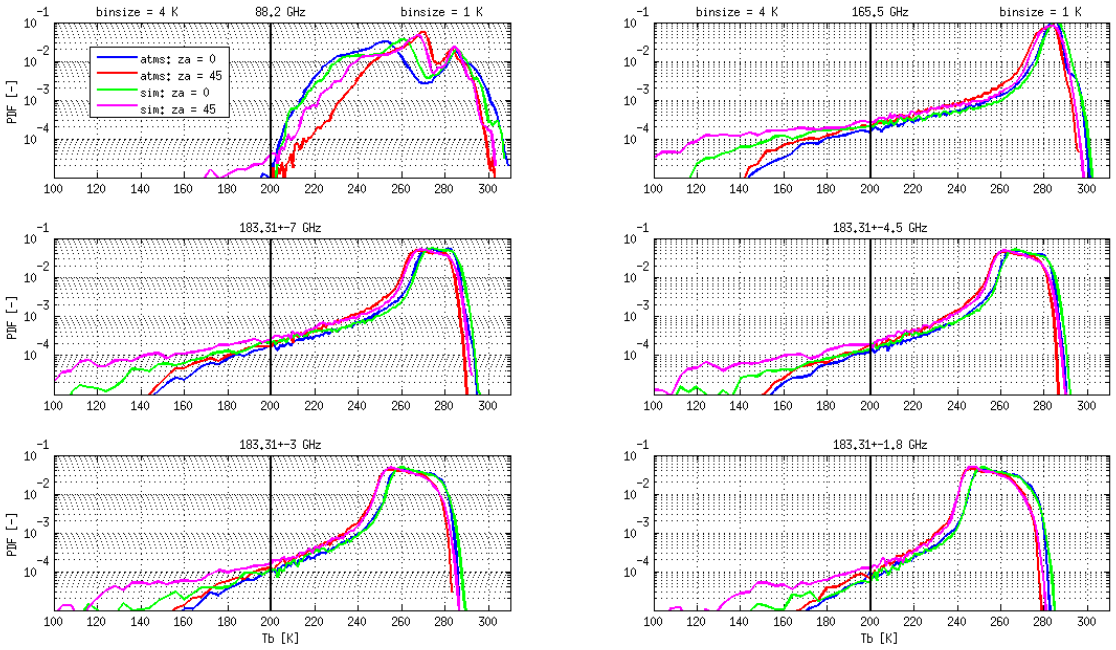

Figure A.5: A statistical comparison of simulated and real ATMS measurements (channel 16–21), for both nadir and slant view (zenith angle of 135° as ICI) observations, between 15° S to 15° N for August 2015.

deviation can possibly also be due to that the assumed microphysics (particle shape and size distribution) are not correct for deep convection cores. Four different ice particle habits are used in this simulation. The more compact particle types (hail and sector snowflake) effectively generates a higher ΔTb than the aggregates for a given amount of cloud ice. A possible explanation is therefore that a too large fraction of compact particle types were used in the simulation. However, a more detailed study is required in order to completely understand this disrepancy.

For ATMS channel 16 (88.2 GHz) the agreement is a bit poorer than for the other channels. This channel is less sensitive to cloud ice due to its lower frequency. Furthermore, it is more complicated to simulate, as this is a window channel, heavily sensitive to the surface emissivity and low level liquid clouds (in particular over ocean where the surface emissivity is low).

Overall, the agreement between observations and simulations werejudged to be high, although some important differences were found, which should be sorted out before the generation of the final ICI retrieval database.

A.5 Data file format

Table A.2: anticipated file format of the ICI training database file. See also Section 2 for a more detailed description of variables.

Name	Type	Dim.	Unit	Description
dtb_ch_1	single	1-D array	K	Simulated cloud signal of ICI channel 1.
dtb_ch_2	single	1-D array	K	Simulated cloud signal of ICI channel 2.
...	...	...	...	...
dtb_ch_11	single	1-D array	K	Simulated cloud signal of ICI channel 11.
od_ch_1	single	1-D array	[−]	Cloud optical depth of ICI channel 1.
od_ch_2	single	1-D array	[−]	Cloud optical depth of ICI channel 2.
...	...	...	...	...
od_ch_11	single	1-D array	[−]	Cloud optical depth of ICI channel 11.
weight	single	1-D array	[−]	a priori weight.
iwp	single	1-D array	kg/m^2	Ice water path. The vertical column, along the slant direction, of atmospheric ice including ice, snow, and hail.
lwp	single	1-D array	kg/m^2	Liquid water path. The vertical column, along the slant direction, of atmospheric liquid water content in cloud.
rwp	single	1-D array	kg/m^2	Rain water path. The vertical column, along the slant direction, of atmospheric rain water content.
cwv	single	1-D array	kg/m^2	Total Column Water Vapour. The vertical column, along the slant direction, of atmospheric water vapor.
zcloud	single	1-D array	m	Mean cloud height by mass.
dmean	single	1-D array	m	Mean particle size by mass, in terms of a mass equivalent spherical diameter.
surface_pressure	single	1-D array	Pa	surface pressure of simulation.
surface_temperature	single	1-D array	K	Skin temperature of simulation.
surface_wind_speed	single	1-D array	m/s	Surface wind speed of simulation.

surface_type	int8	1-D array	[−]	Surface type for simulation: Possible types: 1. water: 0 2. ice: 1 3. mixed: 2 4. land: 3
icehabit	int8	1-D array	*N/A*	The ice particle model identifier used in the simulation: Current habits: (See Table A.1) 1. 11 2. 13 3. 14 4. 21 5. 23 6. 24

Table A.2 describes the anticipated format of the ICI retrieval training database file. The file contain information of cloud signals and a description of the underlying atmospheric and surface variables for each database state.

Appendix B

Retrieval performance sensitivity

B.1 Effect on retrieval using surface parameter data for database filtering

Surface parameter data (temperature, pressure, wind speed, and land sea mask) for the geolocation of the observation are used as a priori data in the retrieval algorithm as described in Sect 3.4.2. In short, only database states with similiar surface data as a given observation are used in the retrieval calculation. This forces the retrieval to produce a physical reasonable output, as the retrieval calculation effectively interpolates between the database states considered. For example, the retrived cloud height will typically be above ~ 6 km if the surface temperature is around 300 K since the cloud height is above ~ 6 km of most database states having a surface temperature around 300 K.

Estimated retrieval performance characteristic for various combinations of "filters" for database state extraction is shown in Table B.1. The retrieval performance is somewhat state dependent and Table B.1 shows retrieval simulation results for states with an IWP around 0.1 and $1\,kg/m^2$. Table B.1 shows that retrieval uncertainties can be significanlty descreased by using surface temperature information in the retrieval. This is in particular true for cloud height (Zmean) where the $\pm 1\sigma$ uncertainty is around 550 m and 780 m for a "hard" and "soft" filter, respectively, and that is almost a 40 % improvement. The IWP $\pm 1\sigma$ uncertainty also improves with surface data filtering (up to 15 % smaller uncertainty).

Table B.1 indicates that also the surface pressure filtering has a positive impact on retrieval performance, although the IWP and Zcloud $\pm 1\sigma$ uncertainties are only a few percent better for a hard than soft filter. However, surface pressure filtering is of particular importance for regions with high surface altitude, while the data displayed in Table B.1 represent average performance.

The use of surface wind speed for filtering data is only anticipated to be of importance for ocean pixels, as wind speed is one of the key component of driving the ocean surface emissivity. Thus, it is of importance to filter (wind speed) database states for ocean pixels in order to not potentially biasing the retrieval (i.e map strong wind to an IWP).

Table B.1: Estimated effect of using surface temperature and pressure as *a priori* data on retrival uncertainties (determined from averaged result of retrieval simulation for states having an IWP around 0.1 and 1 kg/m^2).

Accepted temperature deviation [K]	Accepted pressure deviation [hPa]	IWP bias [%]	IWP $\pm 1\,\sigma$ uncertainty [%]	IWP $\pm 2\,\sigma$ uncertainty [%]	Zmean bias [m]	Zmean $\pm 1\,\sigma$ uncertainty [m]	Zmean $\pm 2\,\sigma$ uncertainty [m]
2	5	-9 / -1	47 / 33	76 / 54	20 / 0	560 / 410	920 / 690
2	10	-7 / -1	46 / 32	75 / 55	20 / 0	550 / 410	920 / 690
2	20	-7 / -1	48 / 33	79 / 55	20 / 0	560 / 410	920 / 710
2	100	-7 / -1	48 / 33	79 / 54	20 / 0	570 / 410	940 / 710
4	5	-8 / -1	48 / 33	78 / 55	20 / 0	570 / 420	960 / 730
4	10	-7 / -1	48 / 33	78 / 55	60 / 0	590 / 420	990 / 730
4	20	-7 / -1	47 / 34	77 / 56	50 / 0	590 / 430	990 / 750
4	100	-8 / -1	47 / 34	79 / 56	50 / 0	600 / 430	1000 / 740
8	5	-9 / -1	50 / 35	81 / 56	40 / 0	640 / 470	1010 / 790
8	10	-8 / -1	49 / 34	79 / 57	20 / 0	660 / 490	1010 / 820
8	20	-8 / -1	49 / 35	79 / 57	40 / 0	670 / 500	1110 / 830
8	100	-8 / -1	50 / 34	81 / 57	30 / 0	680 / 500	1110 / 810
16	5	-7 / -1	51 / 35	88 / 56	0 / 0	700 / 510	1210 / 890
16	10	-7 / -1	51 / 35	83 / 59	0 / 0	750 / 550	1230 / 920
16	20	-9 / -1	51 / 35	87 / 59	0 / 0	770 / 560	1310 / 950
16	100	-9 / -1	53 / 33	87 / 58	0 / 0	780 / 530	1330 / 930

Table B.2: Single channel retrieval performance estimate (see Fig. B.1 for more detailed result).

channel	"Valid" IWP range $[kg/m^2]$	Precision [%]
ICI-1 (183.31 ± 7.0 GHz)	0.25 – 3	200
ICI-4 (243.2 ± 2.5 GHz)	0.15 – 2	200
ICI-5 (325.15 ± 9.5 GHz)	0.06 – 1	300
ICI-8 (448.0 ± 7.2 GHz)	–	–
ICI-11 (664.0 ± 4.2 GHz)	0.03 – 0.08	>300

B.2 Single channel IWP retrieval performance assessment

The ICI retrieval algorithm contains a sub-algorithm where channels can be removed (one by one in a defined order) from retrieval calculation if there is no or few database matches. Thus, there is a possibility that only one channel will be used in the retrieval calculation and in this section the single channel IWP retrieval is assessed in order to provide a guidance how to prioritize the various channels.

Figure B.1 and Table B.2 show single channel IWP retrieval performance simulation result for ICI channels: ICI-1 (183.31 ± 7.0 GHz), ICI-4 (243.2 ± 2.5 GHz), ICI-5 (325.15 ± 9.5 GHz), ICI-8 (448.0 ± 7.2 GHz), and ICI-11 (664.0 ± 4.2 GHz) and Table B.3 provides information on below which temperature the various channels have sensitivy.

It can be seen that single channel retrievals are valid for quite different IWP ranges for the various channels (the various channels also have sensitivity to different altitude layers of the atmosphere). Therefore, it is not straight forward to tell which channel that provides best retrieval result. Anyhow, ICI-1 and ICI-4 are most important for "high IWP" observations. ICI-8 and ICI-11 are most important for "high cloud height and low IWP" observations, but the retrieval precision is low which can be explained by the fact that these channels have low sensitivity to the lower part of the atmosphere, and therefore must rely on a priori data at low altitudes. Thus, these channels alone are not well suited to estimate IWP, as much of the total cloud ice tends to be found at relatively low altitude.

The result shown in this section support the idea that the single channel IWP retrieval is more meaningful for a channel that have sensivity to a large part of atmosphere (e.g. ICI-4) than a channel that have high sensitivity to cloud particle scattering but only a limited sensitivity to cloud ice in the lower part of the atmosphere (e.g. ICI-11). The most meaningful single channel IWP retrieval is obtained from ICI-1, ICI-4, and ICI-5 retrievals, whereas ICI-8 and ICI-11 alone provide less useful results. Furthermore, it is most likely that the true IWP is high for situations when the retrieval algorithm end up with using only channel (see e.g. Fig. 3.8). A natural way to sort the channels (in terms of channel priority) is then according to atmospheric opacity as is done in Table B.2.

It should be clear that the result shown in this section only gives limited information about the usefulness of the various channels in a multi channel IWP retrieval, as the signal from

Table B.3: ICI channels sorted according to clear sky optical depths. The table shows typical surface temperatures that corresponds to a clear sky optical depth of three for the various ICI channels. Table shows for example that ICI-4 and ICI-11 only have a non-negligible sensitivity to the surface if surface temperature is below 290 K and 240 K, respectively (see Table B.4 for more detailed information).

channel	lowest surface temperature [K]
ICI-4	290
ICI-1	280
ICI-5	280
ICI-2	270
ICI-6	270
ICI-3	260
ICI-7	250
ICI-11	< 240
ICI-8	< 240
ICI-9	< 240
ICI-10	< 240

Table B.4: Fraction of database state with a clear sky optical depth greater than three for various surface temperature ranges.

channel	240 - 250 K [%]	250 - 260 K [%]	260 - 270 K [%]	270 - 280 K [%]	280 - 290 K [%]	290 - 300 K [%]	300 - 310 K [%]
ICI-1	0	0	0	4.7942	63.6698	99.5236	100.0000
ICI-2	0	0.1531	14.0315	75.1033	99.8097	100.0000	100.0000
ICI-3	5.3440	25.6413	79.1581	98.9404	100.0000	100.0000	100.0000
ICI-4	0	0	0	0	1.1342	50.0486	99.8608
ICI-5	0	0	0.0039	19.5902	89.5508	99.9814	100.0000
ICI-6	0	4.5709	38.5808	93.2680	99.9800	100.0000	100.0000
ICI-7	33.7341	65.2769	97.3090	99.9317	100.0000	100.0000	100.0000
ICI-8	95.9475	98.9904	100.0000	100.0000	100.0000	100.0000	100.0000
ICI-9	100.0000	100.0000	100.0000	100.0000	100.0000	100.0000	100.0000
ICI-10	100.0000	100.0000	100.0000	100.0000	100.0000	100.0000	100.0000
ICI-11	81.0733	96.7494	99.9715	100.0000	100.0000	100.0000	100.0000

combination of different channels provides useful information.

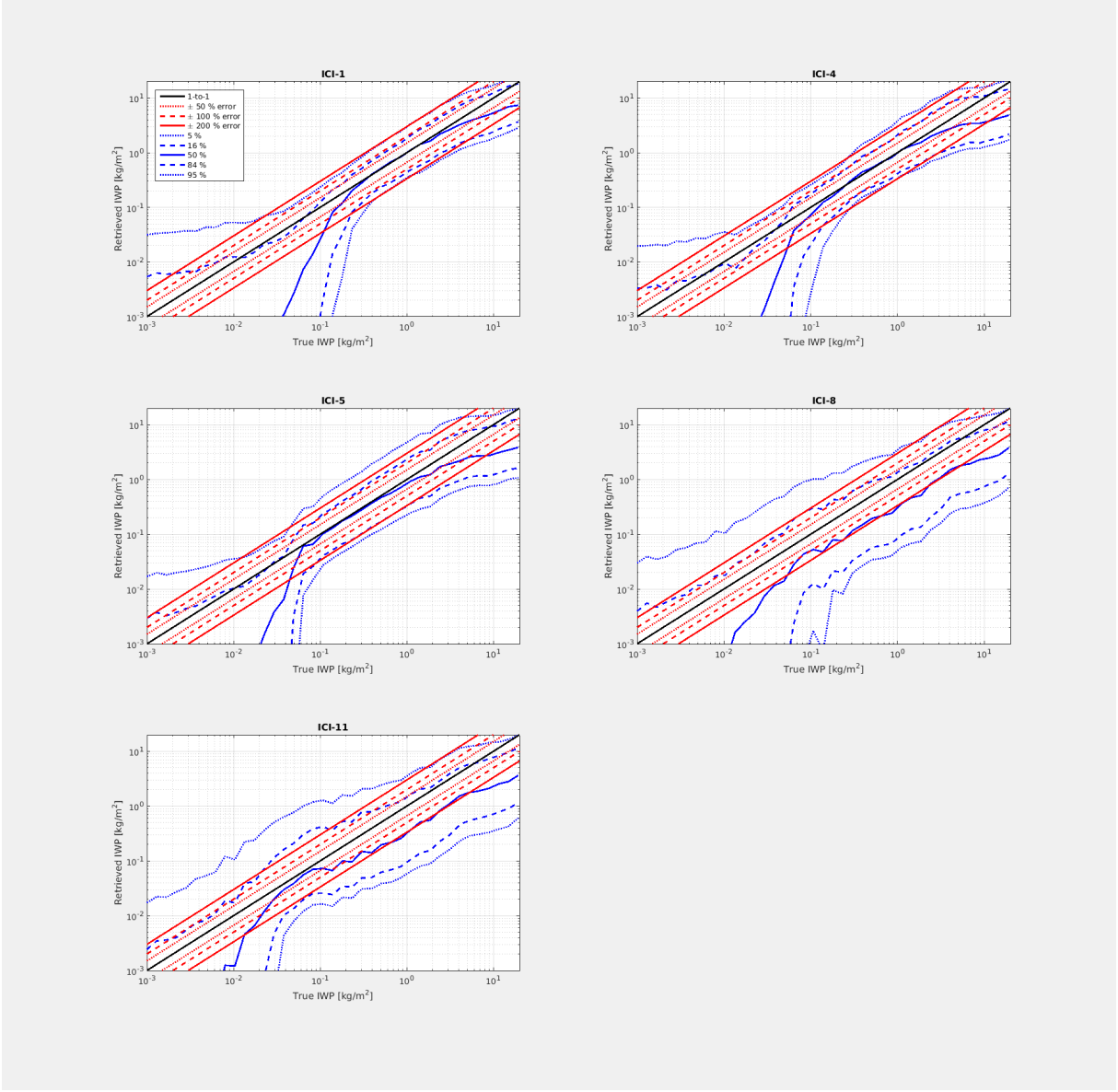

Figure B.1: Single channel IWP retrieval performance simulation result.

B.3 Land / water surface sensitivity

Retrieval uncertainties related to topography and surface emissivity are greater for observations over land than ocean surfaces, and the retrieval algorithm uses information from channels with a possible non-negligible surface contribution in a restrictive manner. Figure B.2 shows estimated retrieval performance of IWP and Zmean separated by surface type (land or water). It can clearly be seen that the retrieval characteristic is better for observations over a water surface than over land surfaces. This is particluarily true for states with a low Zmean (4[km] and below), where the Zmean uncertainity tends to be 1[km] greater over land than ocean surfaces. This indicates that the sensitivity to low altitude cloud ice mass is low over land surfaces and this is clearly a consequence of the limited usability of channels with sensitivity to the surface and lowest part of the atmosphere. A limited sensitivity to low altitude cloud ice mass obviously also impacts the IWP retrieval performance and Fig. B.2 shows that the "water" IWP retrieval uncertainties are significantly lower than "land" uncertainties.

B.4 Effect on retrieval using new channel selection

The retrieval algorithm uses information from channels with a possible non-negligible surface contribution in a restrictive manner. The retrieval calculation is done in an iterative way, where the first calculation only uses information from channels that have a low surface contribution for clear sky condition. A possible second retrieval calculation is performed if already not all channels were used in the first calculation and the retrieved cloud optical depth is high enough to effectively "hide" a possible surface contribution error (see Eq. 3.30).

Figure B.3 shows retrieval performance simulation result with and without a second retrieval calculation, for states with a surface temperature between 270 to 280 K and considering both land and water surfaces (using c=8, $\tau_{min,water}$=1, and $\tau_{min,land}$=3 in Eq. 3.30). ICI channels ICI-1, ICI-4, and ICI-5 are often not included in the first retrieval for those conditions (see Table B.4) over land, where only channels with a clear sky optical depth above three are used.

Figure B.3 shows that a second retrieval is performed for about 80 % of the states having a true IWP above $0.2 kg/m^2$ and for less than 20 % of the states having a true IWP below $0.01 kg/m^2$. This is roughly the intended behaviour of the algorithm, although, these numbers are not general as they for example depends on the the initial channel selection and clear sky optical depth. For example, in the tropical region all channels are anticipated to be used in the first retrieval most often, and a second retrieval is therefore not needed.

Anyhow, Fig. B.3 shows that the retrieval performance improves by including a second retrieval calculation. For example, the 95 % and 5 % pair of CDF values for an IWP around $1 kg/m^2$ is ($0.7 kg/m^2$ and $1.7 kg/m^2$) and ($0.6 kg/m^2$ and $1.9 kg/m^2$) for a first and second retrieval, respectively. This is a $0.3 kg/m^2$ or 25 % decrease of the range. Decreased error uncertainties are found throughout the complete range of IWP values, and not only for states with high IWP as might be expected. This can be explained by that the added channel will provide increased information about the vertical distribution of cloud ice mass.

It is also a possibility that the second retrieval calculation will result in a retrieval where fewer channels were used than in the first one (due to a possible recovery iteration). The retrieval performance for such cases anyhow tend to improve (by applying a second retrieval) as

the channels ultimately used then have a greater sensitivity to the lower part of the atmosphere, where potentially a large fraction of the cloud ice can be found.

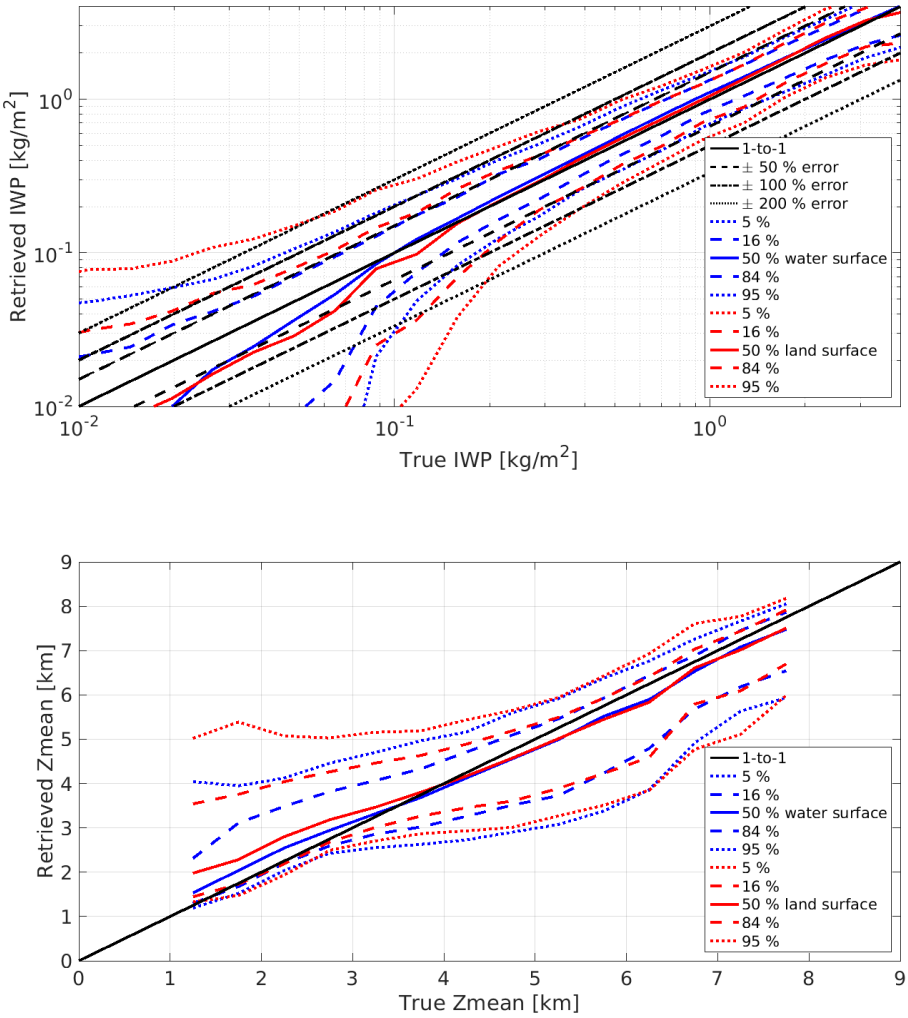

Figure B.2: Retrieval performance simulation results separated by surface type (land or water) for states having a surface temperature between 270 – 280 K. Upper and lower panel show result for IWP and Zmean, respectively.

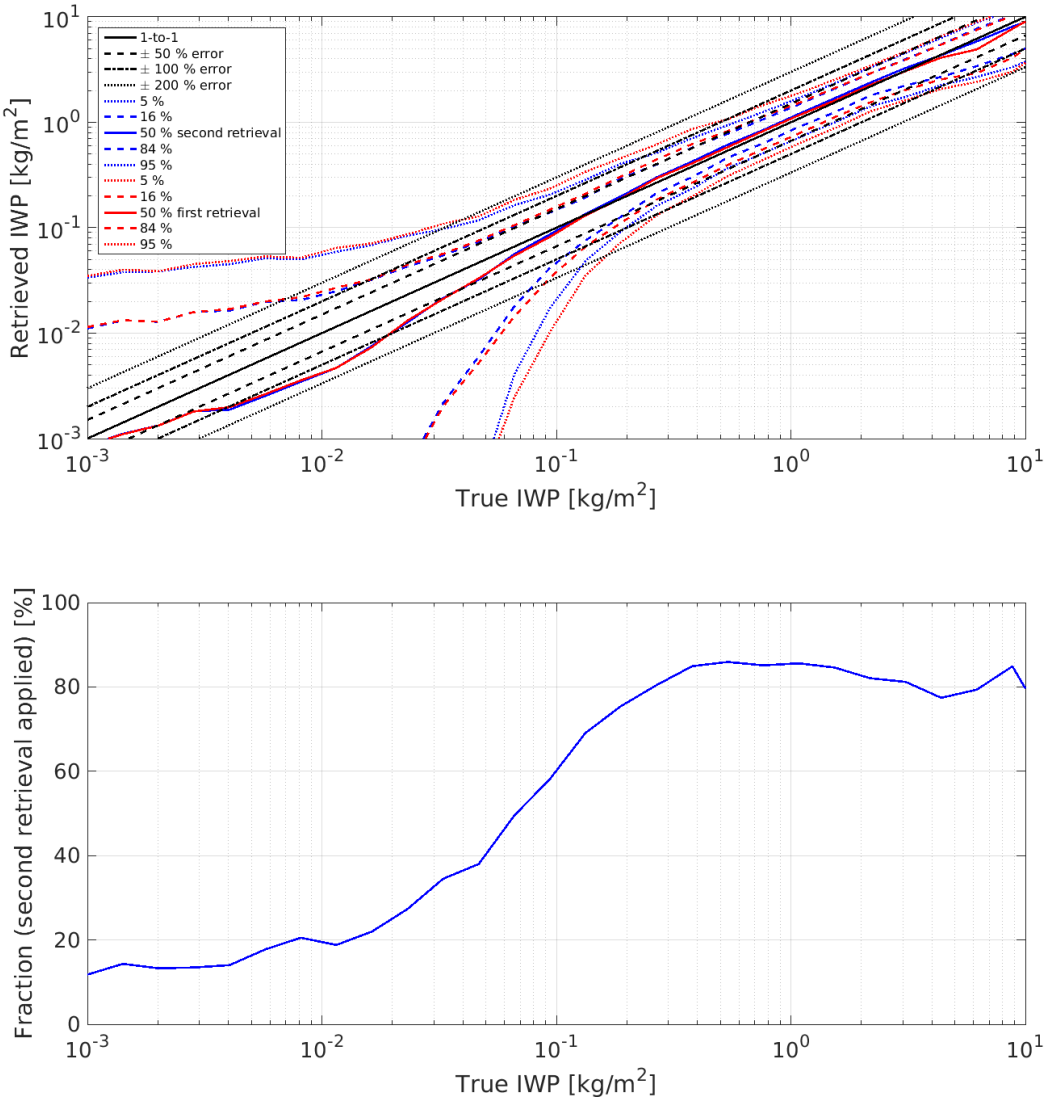

Figure B.3: Retrieval performance simulation results by excluding or including a second retrieval. See text for more details.

Appendix C

Test of ICI retrieval algorithm

C.1 Application on GMI observations

The ICI level2 retrieval algorithm has been applied on observations from the Global Precipitation Measurement (GPM) Microwave Imager (GMI). The main aim of this exercise (high level test) was to verify that the algorithm works as anticipated w.r.t. to the IWP retrieval. More specifically, the aim was to confirm that retrieved IWP pattern, including the error estimates, are reasonable.

The application of the algorithm on GMI observation was considered because GMI is probably the most similar satellite instrument to ICI that is in service today, if both the deployed channels and scanning pattern are taken into account.

The Global Precipitation Measurement (GPM) Microwave Imager (GMI) instrument is a multi-channel, conical scanning, microwave radiometer. GMI has thirteen microwave channels ranging in frequency from 10 GHz to 183 GHz. The satellite was launched at 2014-02-27 into a circular, non-sun-synchronous orbit an altitude of 407 km, and with an inclination of 65 ° to the equator. The off-nadir-angle defining the cone swept out by the GMI is set at 48.5 ° which represents an earth-incidence-angle of 52.8 °. GMI gathers microwave radiometric brightness measurements over a 140 ° sector centered about the spacecraft ground track vector, which gives a swath of around 900 km at the Earth's surface. With a 1.2 m diameter antenna the footprint resolution is around 5 km for the highest frequency channels.

The ICI level2 retrieval algorithm was applied on GMI observation for a scene centered around 2015-09-02T06:07Z and using GMI channels 11, 12, and 13 (166.0 GHz, 183.31 ± 3 GHz, 183.31 ± 7 GHz). Figures C.1, C.2, and C.3 show the observed brightness temperatures and retrieved IWP values (low, high, and best IWP estimate, respectively) for the scene. The figures display also a collocated infrared (IR) image collected from a geostationary satellite. This scene was selected, for this exercise, as it contains some interesting features or patterns that vary over different scales. Observed GMI brightness temperatures are very cold (below 100 K and outside the color scale), for the considered channels, for the heavy cloud structure centered around a latitude of $5\,°N$. Outside this region various pattern can be seen in GMI observation.

The IWP estimate of Fig. C.1 has the meaning that there is a 95 % probability that IWP is above this value and can seen as clear cloud detection. It can be seen that these clear cloud

detection, in principle, only occur at locations where GMI observation (and the IR image) shows very cold temperatures. This indicates that the algorithm is capable of identifying clear cloud detection in a reasonable manner.

Fig. C.2 shows an estimate of the highest possible IWP of the scene (there is 95 % probability that IWP is below this value). It can be noted that the region with an IWP estimate greater than 0.01 kg/m^3 shows a high level of agreement to observed brightness temperatures of the 183.31 ± 3 GHz and 183.31 ± 7 GHz channels. Pixels where the 183.31 ± 3 GHz and 183.31 ± 7 GHz channels observes brightness temperatures lower than approximately 260 K and 270 K, respectively, are given an IWP estimate greater than 0.01 kg/m^3. Pixels where brightness temperatures are above this level is basically given a 0 kg/m^3 IWP estimate. Part of region which where given an IWP estimate greater 0.01 kg/m^3 are not obviously cloudy according to the IR image, since some of these pixels shows relatively high temperatures in the IR image. The true IWP for these pixels are probably around 0 kg/m^3. The reason for such discrepancies can be explained by the much lower sensitivity to clouds by the GMI observation compared to IR observation. Overall, this high IWP estimate shows a reasonable behavior.

Figure C.3 shows the retrieved median IWP (best estimate) of the scene. Pixels that are given an IWP greater than 0.01 kg/m^3 are correlated to pixels where observed brightness temperature are below about 255 K and 265 K for the 183.31 ± 3 GHz and 183.31 ± 7 GHz channels, respectively. It can also be noted that there is a high level of agreement between the retrieved IWP pattern and the IR image. High IWP estimates are found where the IR image shows low temperatures ($\sim$-70 – -50 K), and intermediate IWP values are found where IR values are around -30 K.

Overall, this comparison test shows a positive indication that the IWP error estimates as returned by the ICI level2 retrieval algorithm are reasonable. The actual sensitivity to clouds presented in this comparison test is not valid for ICI, as ICI will indeed have a much higher sensitivity to clouds than GMI.

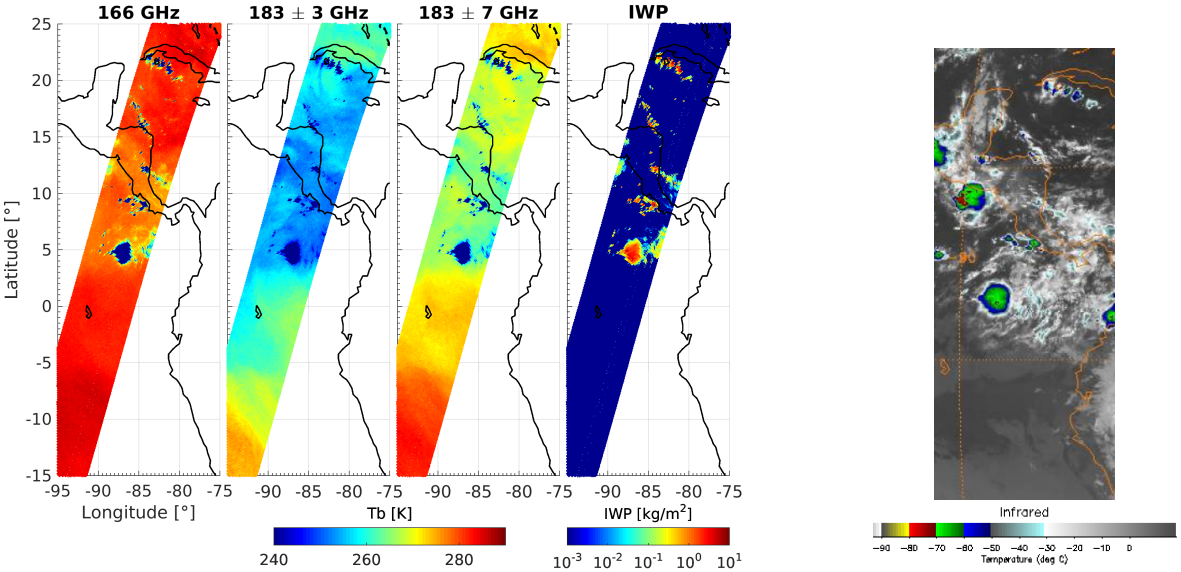

(a) (b)

Figure C.1: (a) Observed brightness temperatures by GMI channel 11, 12, and 13, and retrieved IWP (low estimate) by the ICI level2 retrieval algorithm for a scene centered around 2015-09-02T06:07Z. (b) Infrared image (10.5 μm) collected from a geostationary satellite around 2015-09-02T06:00Z.

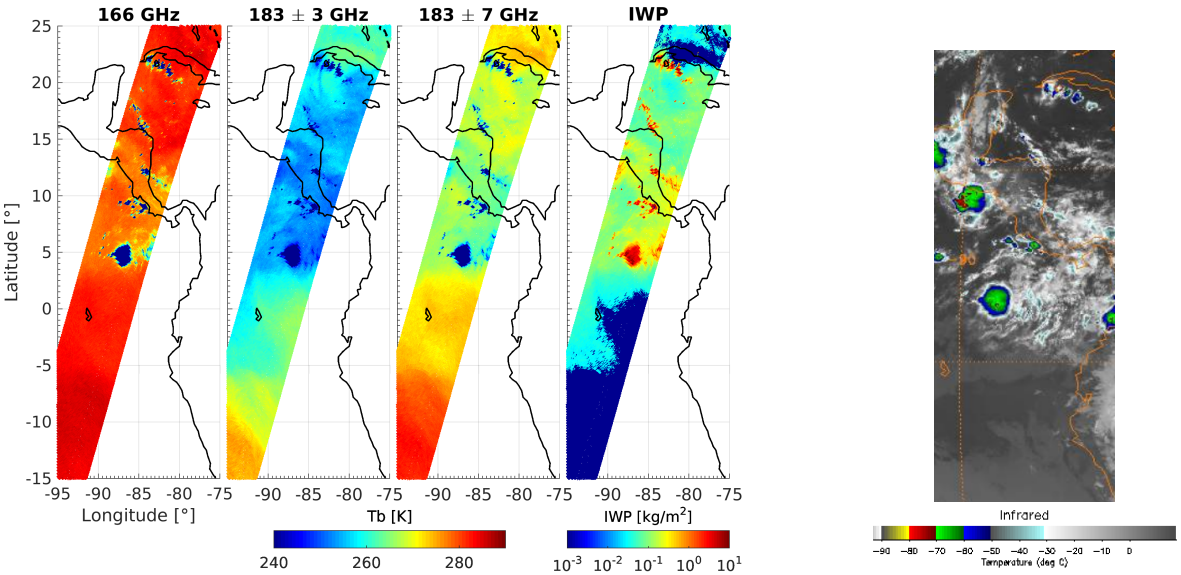

(a) (b)

Figure C.2: (a) Observed brightness temperatures by GMI channel 11, 12, and 13, and retrieved IWP (high estimate) by the ICI level2 retrieval algorithm for a scene centered around 2015-09-02T06:07Z. (b) Infrared image (10.5 μm) collected from a geostationary satellite around 2015-09-02T06:00Z.

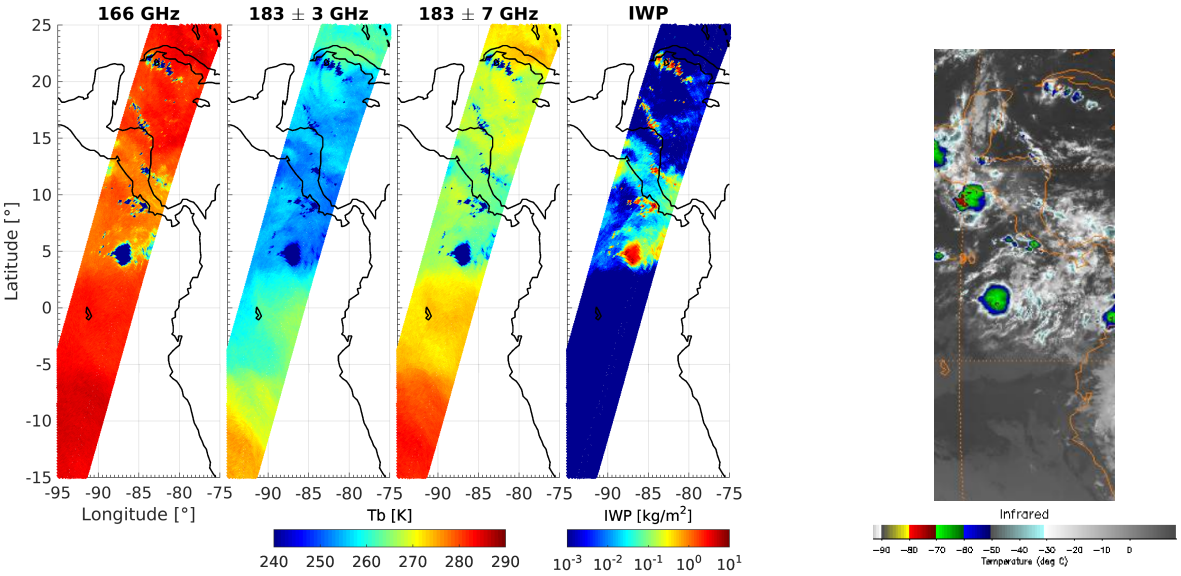

(a) (b)

Figure C.3: (a) Observed brightness temperatures by GMI channel 11, 12, and 13, and retrieved IWP (best estimate) by the ICI level2 retrieval algorithm for a scene centered around 2015-09-02T06:07Z. (b) Infrared image (10.5 μm) collected from a geostationary satellite around 2015-09-02T06:00Z.

C.2 Application on ISMAR / MARSS observations

ISMAR/MARSS

ISMAR (International SubMillimetre Airborne Radiometer) is an airborne demonstrator instrument for ICI. ISMAR was designed to be mounted on the FAAM BAe-146 research aircraft. ISMAR has been flown together with other instruments, e.g. MARSS (Microwave Airborne Radiometer Scanning System), for a number of flights. An early version of ICI retrieval algorithm / database (slightly different from what is currently described in this document) has been applied on combined ISMAR and MARSS measurements and some results are presented in this section.

Table C.1 describes the considered ICI and MARSS channels, which is similar to the ICI channels (the main difference is the ISMAR 118.75 GHz channels which ICI will not have). ISMAR and MARSS are both scanning instruments and can view scenes with several angles (from both above and below). However, here we only consider measurements when the flight altitude is around 10 km and the viewing direction is similar to that of ICI.

Table C.1: ISMAR and MARSS instrument characteristics for considered channels.

Channel Name	Instrument	Frequency [GHz]	Polarisation
IM-1	ISMAR	118.75 ± 1.1	V
IM-2	ISMAR	118.75 ± 1.5	V
IM-3	ISMAR	118.75 ± 2.1	V
IM-4	ISMAR	118.75 ± 3.0	V
IM-5	ISMAR	118.75 ± 5.0	V
IM-6	MARSS	183.31 ± 1.0	V
IM-7	MARSS	183.31 ± 3.0	V
IM-8	MARSS	183.31 ± 7.0	V
IM-9	ISMAR	243.20 ± 2.5	V and H
IM-10	ISMAR	325.15 ± 1.5	V
IM-11	ISMAR	325.15 ± 3.5	V
IM-12	ISMAR	325.15 ± 9.5	V
IM-13	ISMAR	448.00 ± 1.4	V
IM-14	ISMAR	448.00 ± 3.0	V
IM-15	ISMAR	448.00 ± 7.2	V
IM-16	ISMAR	664.00 ± 4.2	V and H

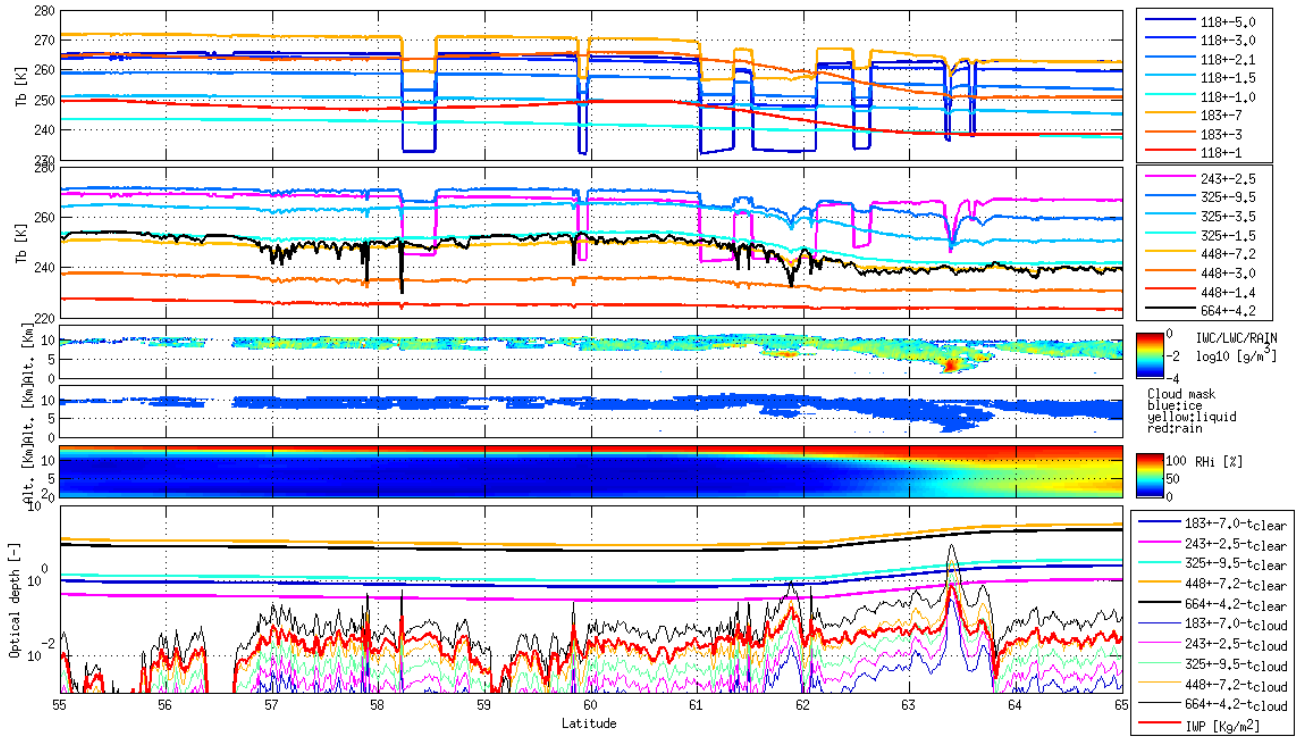

Figure C.4: An example of an atmospheric scene (for mid/high latitude conditions) and measurement simulation. The upper panel shows simulated measurements for ISMAR and MARSS. The second and third panel show cloud water content (in various phases), and cloud phase mask. The bottom panel shows clear sky and cloud optical depths for the outermost 183, 325, and 448 GHz channels, and the 243 and 664 GHz channels, and IWP.

Retrieval performance simulations

Figure C.4 shows a simulated scene for mid/high latitude condition, i.e. an ISMAR / MARSS overflight of a fairly thin and high altitude cloud system (a mean cloud height just below 10 km and an IWP mainly between 0 to 100 g/m^2. Such cloud systems should be close to ideal for ISMAR / MARSS and ICI, and Figure C.5 shows simualted retrieval performance for this scene. The agreement between the retrieved *posteriori* median IWP, D_{mean}, and Z_{mean} and the true values are generally high. The IWP error estimate, as described by the CDF levels corresponding to $\pm 1\,\sigma$ and $\pm 2\,\sigma$, typically have values around ± 10 g/m^2 and ± 25 g/m^2, respectively. The lower error level is sometimes lower, which is explained by the fact that the lowest possible level of IWP is 0.

A more varying (and more challenging for ISMARS / MARSS) scene is displayed in Figure C.6. The IWP and Z_{mean} varies between 0 - 1000 g/m^2 and 1 - 6 km, respectively. Figure C.7 shows simualted retrieval performance for this scene. The agreement between the retrieval and the truth is high for states where the true Z_{mean} is above ∼2 km. For states where Z_{mean} is below ∼2 km. there are significantly differences between retrieved and true IWP, Z_{mean}, and D_{mean}.

The reason for this can be seen in the top panel, which shows the "observed" cloud signal

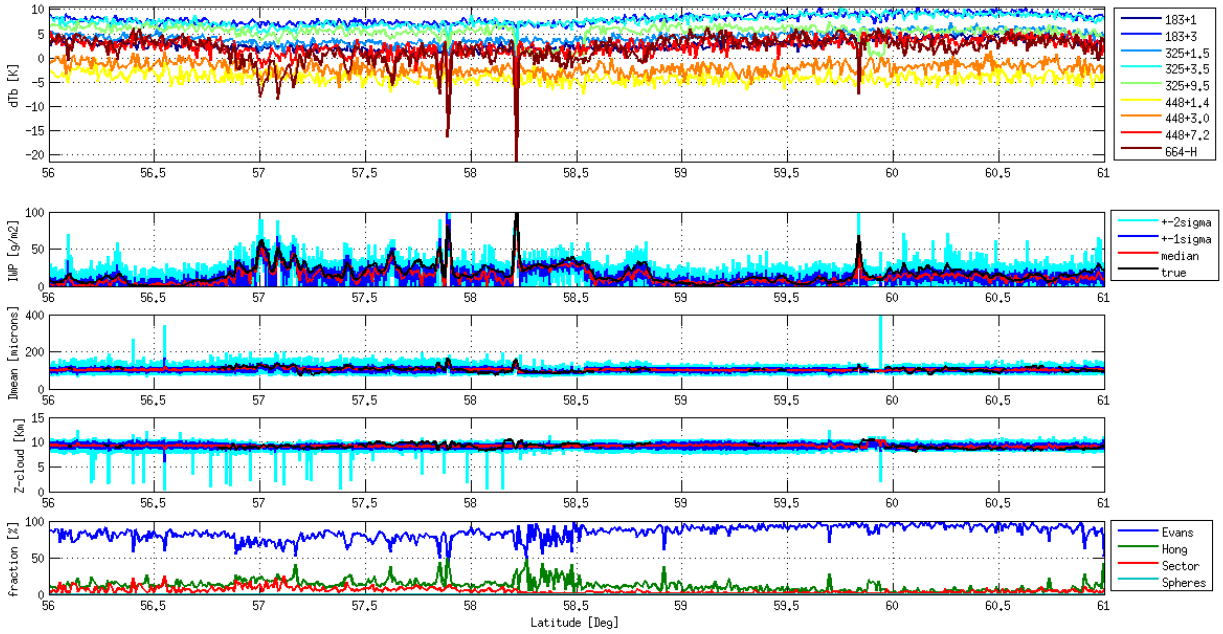

Figure C.5: Retrieval peformance simulation of the scene displayed in Figure C.4. The upper panel shows the "observed" cloud signal for the channels that have low or no sensitivity to the surface. The second to forth panels shows true and retrieved IWP, Z_{mean}, and D_{mean}, respectively. The lowest panel shows retrieved ice particle habit.

for the channels that have low or no sensitivity to the surface. The cloud signal is small, for simulations at a latitude of around 59.5° N, whereas the IWP is above 500 g/m^2. Such high IWP values result in pronounced cloud signals if Z_{mean} is high, but in this case the Z_{mean} is around 1 km, which effectively means that only channels that have a significant surface influence will detect this IWP (see Figure C.6). However, these channels are excluded from the first iteration of the retrieval, and since no other channels detect this IWP, no second iteration of the retrieval is performed.

Thus, states with low Z_{mean} (or states with low level clouds with no higher level clouds above) are problematic, since our limited knowledge of surface modelling force the retrieval problem to be almost impossible to solve accurately, since channels that have sensitivity to the low level clouds are excluded for usage. However, this retrieval artifact is mainly a problem for mid and high latitude winter scenes. The conditions that introduce this difficult retrieval situation should be very rare for mid-latitude summer and tropical conditions.

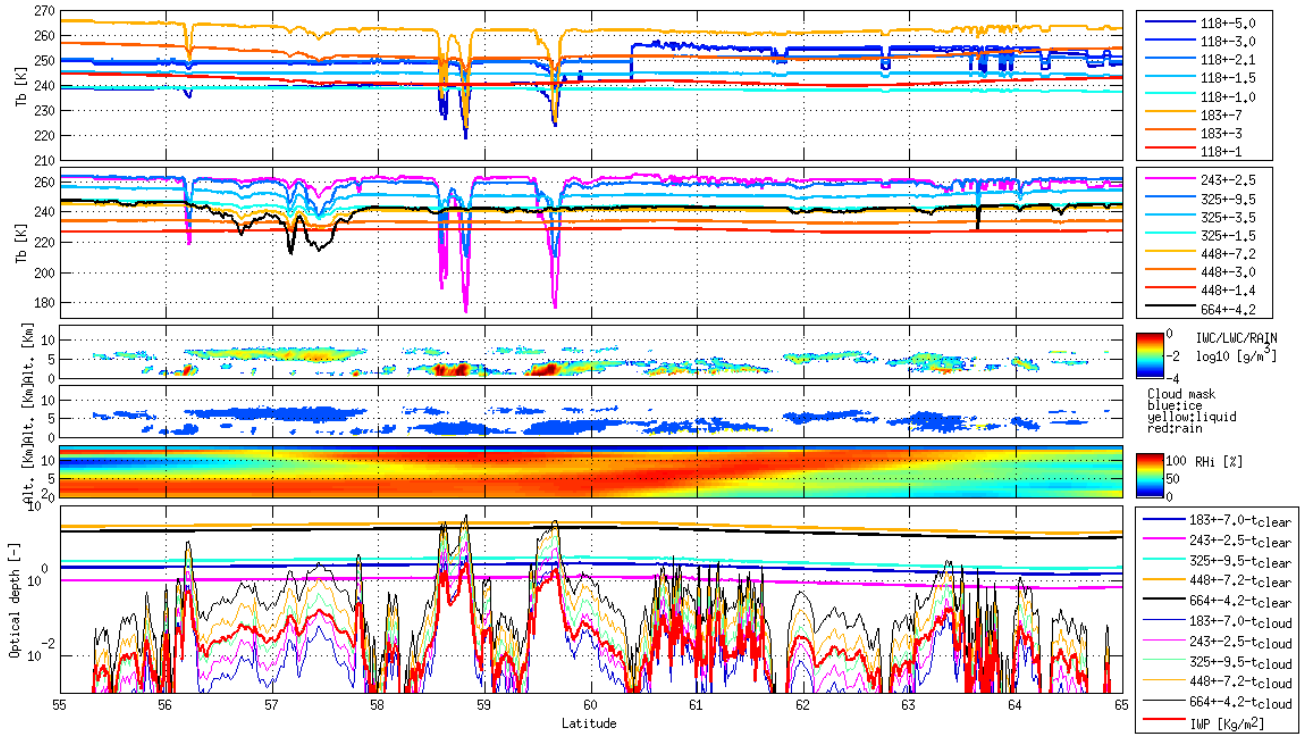

Figure C.6: An example of an atmospheric scene (for mid/high latitude conditions) and measurement simulation. The upper panel shows simulated measurements for ISMAR / MARSS, and the lower panels the underlying atmospheric state. The second and third panel show cloud water content (in various phases), and cloud phase mask, respectively, mainly based on data from the DARDAR Level2 product. The bottom panel shows clear sky and cloud optical depths for the outermost 183, 325, and 448 GHz channels, and the 243 and 664 GHz channels, and IWP. Simulations have been performed for a slant view.

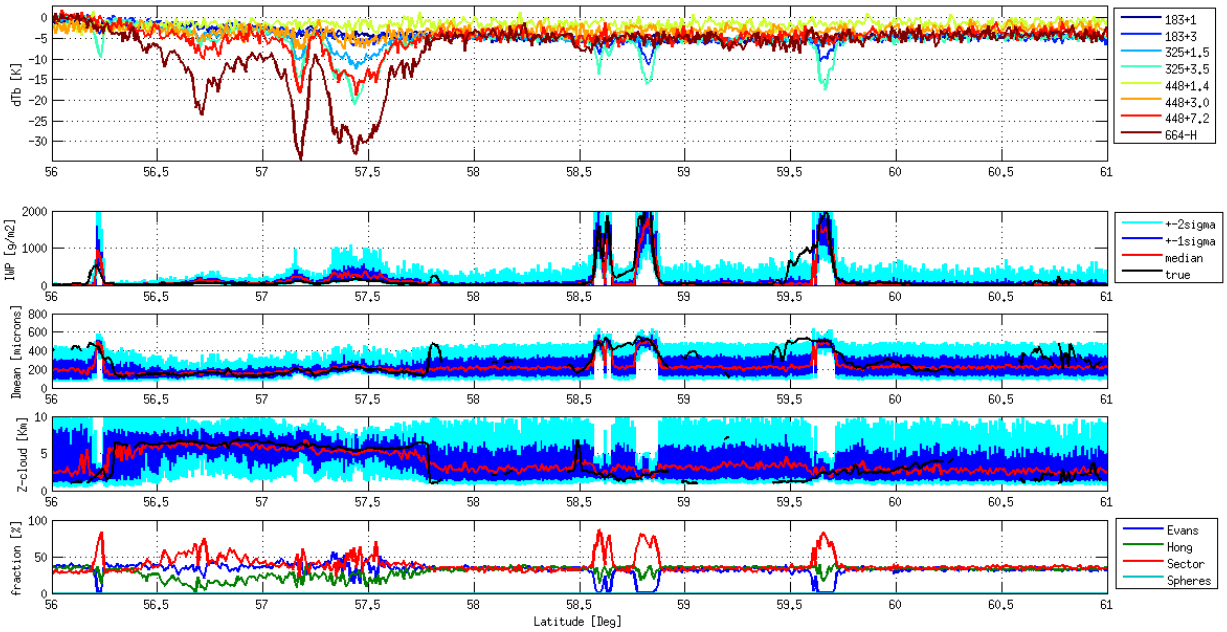

Figure C.7: Retrieval peformance simulation of the scene displayed in Figure C.6. The upper panel shows the "observed" cloud signal for the channels that have low or no sensitivity to the surface. The second to forth panels shows true and retrieved IWP, Z_{mean}, and D_{mean}, respectively. The lowest panel shows retrieved ice particle habit.

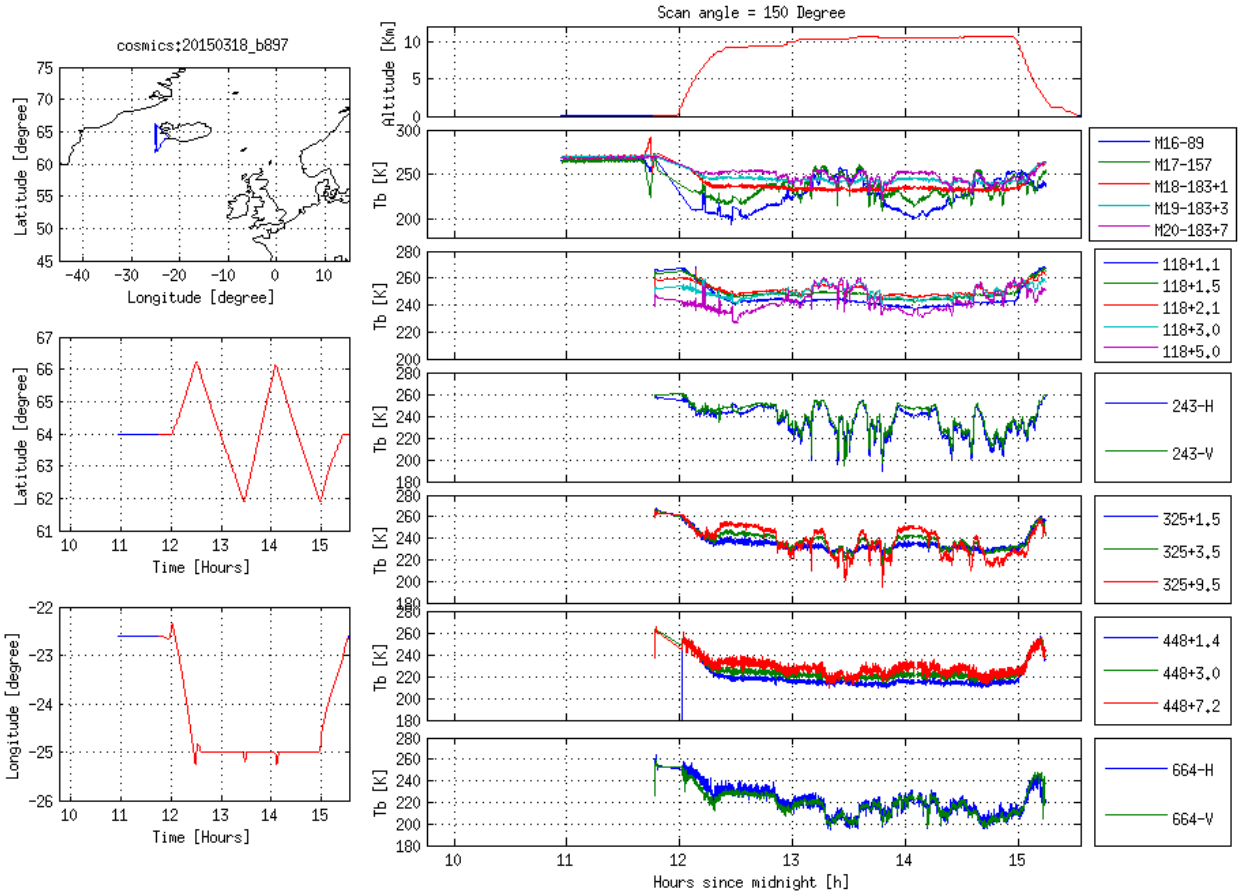

Figure C.8: ISMAR/MARSS measurements from the b897 flight of the Cosmics campaign. The left panels show the geolocation of the flight. The top right panel shows the flight altitude of the FAAM BAe-146 research aircraft. The remaining right panels show timeseries of observed brightness temperatures, for a nominal scanning angle of 130 degree (from zenith), for various frequency bands as indicated in the legends.

Retrieval based on real data

Figure C.8 shows ISMAR/MARSS measurements from a flight that took place west outside of Iceland 2015-03-18 above a low pressure system. Clear "dips" (cloud signals) in the observed brightness temperatures are found in the measurements, although some of the variation in the observed signal is due to changes in flight altitude. For the 325 and 448 GHz channels the strongest cloud signals are found in the outermost bands (w.r.t. to the water vapor transition), which indicates that most of the ice mass of the cloud system are found at a relatively low altitude. However, clear cloud signals are also found in the 664 GHz V and H channels, and thus, not all of the ice of the system is at a low level, since these channels have very low sensitivity to the lower part of the troposphere.

Figure C.9 shows retrieval data from this scene (the truth is not known). The retrieved IWP varies largely (0 - 3 kg/m^2) over the system, and the retrieved Z_{mean} varies between 2.5 - 7.5 km. The anti correlation between retrieved Z_{mean} and D_{mean} is high as expected; states

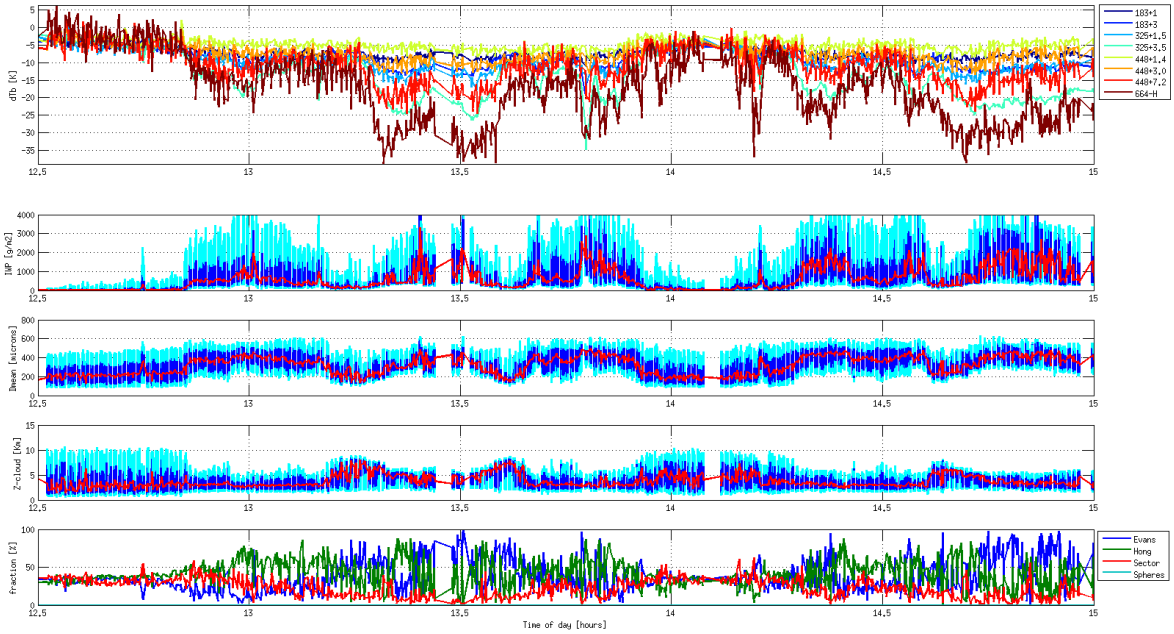

Figure C.9: Retrieval data of the Cosmics B897 flight (Figure C.8). The upper panel shows observed cloud signal of the channels with low or no sensitivity to the surface. The second to forth panels shows retrieved IWP, Z_{mean}, and D_{mean}, respectively. The red, blue, and light blue coloured lines indicate *posteriori* median, and $\pm 1\,\sigma$ and $\pm 2\,\sigma$ retrieval uncertainties. The lowest panel shows retrieved ice particle habit.

with relatively high Z_{mean} have low D_{mean}, and states with low Z_{mean} have high D_{mean}. The uncertainty of the retrieved IWP is considerably high, for most cases and when IWP is well above 0, the $\pm 1\,\sigma$ uncertainty corresponds roughly to -50 % and +100 %.

IWP retrieval performance summary

The descibed ICI retrieval algorithm was applied and tested on ISMAR/MARSS measurements. The retrieval performance of the ISMAR/MARSS combination is anticipated to be very close to the ICI retrieval performance, due to the high similiarity. The IWP retrieval performance was found to be very dependent on the measured atmospheric state. First, for states with an IWP below 100 g/m^2 and with high Z_{mean}, the retrieval uncertainty ($\pm 1\,\sigma$) is in the order of $\pm$10 g/m^2. Second, for states with an IWP well above 100 g/m^2 and with high Z_{mean}, the retrieval uncertainty ($\pm 1\,\sigma$) is in the order of -50 % and +100 %. Third, for states with low Z_{mean} the retrieved IWP can be close to useless, as only the *a priori* IWP is retrieved which corresponds to 0 g/m^2.